J. Fluid Mech. (1988), *vol.* 188, *pp.* 301–335
Printed in Great Britain

The interaction of two spatially resonant patterns in thermal convection. Part 1. Exact 1:2 resonance

By M. R. E. PROCTOR
Department of Applied Mathematics and Theoretical Physics, University of Cambridge, Silver Street, Cambridge CB3 9EW, UK

AND C. A. JONES
Department of Applied Mathematics. University of Newcastle-upon-Tyne, NE1 7RU, UK

(Received 29 May 1987)

The linear stability of two superimposed layers of fluid, heated from below and separated by a thin conducting plate, is investigated. It is shown that when the ratio of the depths of the layers is close to 1:2, two distinct modes of convection can occur with preferred horizontal wavenumber in the ratio 1:2. The nonlinear evolution of a disturbance consisting of both modes is considered, and it is shown that travelling waves are the preferred mode of nonlinear convection for a wide range of parameter values. Other possible types of behaviour, including modulated waves and an attracting homoclinic trajectory, are also described in detail.

1. Introduction

The nonlinear interaction of different spatial structures in convection is a problem whose study has a long history, but which has experienced a resurgence recently, in the attempt to understand the transition to chaos in large fluid layers. The work of Rayleigh (1916) showed that a fluid layer heated from below first became unstable to motions with a definite horizontal wavenumber: early investigations of the nonlinear development of convection (e.g. Malkus & Veronis 1958) were founded on the idea that motions with this preferred horizontal scale (or one nearby) would dominate the dynamics. Indeed, experiments in a fluid layer (Busse & Whitehead 1971) in which motions of a given horizontal scale could be forced initially, and were then found to be stable well into the nonlinear regime, increased the perceived importance of cellular convection patterns, at least in the neighbourhood of the stability boundary. However, the results of experiments *without* initial periodic forcing in a large-aspect-ratio layer (for example, Ahlers & Behringer 1978) showed that regular cellular patterns were metastable at best, with convection generally being quite disordered and exhibiting persistent time dependence even very close to the instability threshold. Theories of these disordered patterns have been attempted in terms of *modulations* of the amplitudes and phases of the rolls (Newell & Whitehead 1968; Cross & Newell 1984; Fauve 1985) but these theories all rely on the dominating influence of the preferred wavenumber. The modulation theory, moreover, takes no account of the absolute value of the phase of the underlying (nearly) cellular structure. Pomeau (1984) has shown that in certain cases (e.g. of abrupt changes in roll orientation) interactions that involve the absolute phase

become important. Furthermore, very recent work of Chaté & Manneville (1987) on a model problem (the so called Kuramoto–Sivashinsky equation)

$$\dot{f} = -\alpha f - f'''' - \mu f'' + ff', \quad \left[f' \equiv \frac{\partial}{\partial x} f(x, t) \right] \tag{1.1}$$

(which can be thought of as a model for convective systems with a preferred wavenumber near the onset of instability) have demonstrated the crucial importance of *travelling waves*, involving several different wavenumbers, in creating the kind of spatial irregularity that by analogy is held to model the 'spatial intermittency' characteristic of large systems far from equilibrium.

It thus seems important to understand the nonlinear interaction of convective modes of different horizontal wavenumber. Analyses in the weakly nonlinear regime have been carried out by Segel (1962, 1965) and more recently by Knobloch & Guckenheimer (1982) and Busse & Or (1986). These papers all treat Boussinesq convection with *symmetric* thermal and mechanical boundary conditions, and show that the interaction between the different horizontal modes (provided the assumed horizontal scale is such that two (or perhaps more) modes become unstable simultaneously) can be described by amplitude equations whose nonlinear interaction terms are *cubic* in the amplitudes at leading order, and take the form

$$\dot{A}_i = \mu_i A_i - A_i \sum_j c_{ij} |A_j|^2, \tag{1.2}$$

where the indices i, j run over all the unstable modes. Thus only the moduli of the A_i are coupled, and their relative phases not determined. More recently F. H. Busse (1987, personal communication), has noted that if the Boussinesq approximation is relaxed so as to allow, for example, non-uniform viscosity and thermal conductivity then extra terms *quadratic* in the amplitude can appear in the equivalent of (1.2) in the special case where two modes with horizontal wavenumbers in the ratio 1:2 become unstable almost simultaneously. These quadratic terms *do* involve the relative phases of A_1 and A_2 and so provide a prototype model for the study of the sort of non-adiabatic effects whose importance Pomeau correctly emphasized. Dangelmayr (1986) was the first to discuss these augmented equations (5.1). Jones & Proctor (1987) gave further results, being motivated by a problem in thermal convection. Independently, Armbruster, Guckenheimer & Holmes (1987) considered the same equations from a group-theoretic point of view, and obtained many mathematical results similar to those given in the present paper. Here, besides presenting a new experimental prototype, we give a full treatment of the derivation of the results presented by Jones & Proctor (1987).

The interactions of these resonant modes in a single layer of fluid depend on careful selection of the allowed wavenumbers. This can be achieved in an annular or cylindrical geometry: but then the interesting effects of amplitude and phase modulation cannot be investigated. In a large-aspect-ratio fluid layer the bifurcations leading to travelling waves can only occur when the convection is fully nonlinear, and analytical methods will not suffice. We therefore decided to study two superimposed layers of fluid, thermally but not mechanically coupled. The top boundary of the upper layer and the bottom boundary of the lower layer are supposed maintained at fixed temperature, while the thin dividing plate can be heated (for example by an electric current), so that the temperature gradients in each layer may be independently varied. Since different working fluids may be used in each layer, and the relative depths of each layer may be varied, this system has

potentially rich behaviour. In §2 we set up the equations for the system, and in §3 solve the linearized stability problem. It is shown that parameter values can be chosen so that two distinct modes of convection, with preferred horizontal wavenumbers in the ratio 1:2, bifurcate simultaneously. In §4 we derive the nonlinear evolution equation for the amplitudes of these two modes, assuming that there is no modulation. The more complicated dynamics that ensues when the preferred modes are not quite in the ratio 1:2 will be deferred to a later paper. Section 5 gives a full discussion of the evolution equations, building on and extending the earlier work of Dangelmayr. In §6 we analyse the different kinds of time-dependent behaviour that can occur, and the important consequences of the presence of imperfections in the system. Finally in a conclusion we examine the implications of the analysis of the evolution equations in §§5 and 6 on our physical problem, and consider the relevance of our findings to other problems.

2. Formulation of the problem

In this and the two subsequent sections we give a full description of the dynamics of a two-layer convection problem. The main thrust of the analysis is the derivation of the evolution equations (5.1). Readers more interested in the general properties of solutions of that equation may pass directly to §5.

We consider two horizontal infinite layers of fluid, one above the other, separated by a thin, conducting, heated plate (see figure 1). We can have either two different fluids in the two layers or the same fluid, but we shall derive the equations on the basis of two different fluids and treat the one-fluid situation as a special case. We take the depth of the lower layer to be d, and of the upper layer to be d/D, so that D is the depth ratio of the two layers. We assume that the lower surface is held constant at temperature T_b and the upper surface at T_u, $T_b > T_u$. The intermediate plate at $z = d$ supplies a uniform heat flux F_0. The heat flux through the system is controlled by two adjustable parameters, the heat flux F_0 and the temperature difference between the lower and upper boundaries $T_b - T_u$. The presence of two adjustable parameters is important because, as we shall see below, the most interesting phenomena occur when the two layers are both near the threshold of the onset of convection. Both parameters have to be correctly adjusted to achieve this situation.

We assume the fluids have kinematic viscosity ν_k, thermal diffusivity κ_k and coefficient of expansion α_k, $k = 1$ referring to the lower layer and $k = 2$ to the upper layer. Because of the jump in the heat flux at the intermediate plate, whose temperature we take to be T_m, we have

$$\frac{D\kappa_2(T_m - T_u)}{d} = \frac{\kappa_1(T_b - T_m)}{d} + F_0,$$

so that

$$T_m = \frac{\kappa_1 T_b + D\kappa_2 T_u + F_0 d}{\kappa_1 + D\kappa_2}. \tag{2.1}$$

It is clear that T_m will exceed T_b if $F_0 > (T_b - T_u) D\kappa_2/d$. If F_0 exceeds this value, the lower layer will be stably stratified, which is not the situation we are interested in here, so we shall assume that $F_0 < (T_b - T_u) D\kappa_2/d$, so that $T_b > T_m > T_u$. We can now define Rayleigh numbers for the two layers:

$$R_1 = \frac{g\alpha_1(T_b - T_m) d^3}{\kappa_1 \nu_1}, \quad R_2 = \frac{g\alpha_2(T_m - T_u) d^3}{D^3 \kappa_2 \nu_2}. \tag{2.2}$$

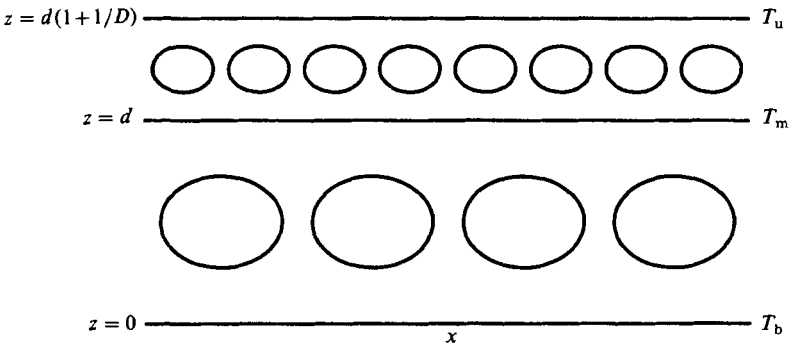

FIGURE 1. Sketch of the experiment.

As the flux increases from 0 to $(T_b - T_u) D\kappa_2/d$, R_1 decreases steadily while R_2 increases steadily. Provided

$$\alpha_1 \kappa_2^2 \nu_2 D^4 > \alpha_2 \kappa_1^2 \nu_1 \tag{2.3}$$

it is possible to choose a value of F_0 so that $R_1 = R_2$. As we see below, the condition for the simultaneous onset of convection in both layers is not exactly at $R_1 = R_2$, because of the thermal coupling between the layers through the intermediate plate, but the numerical results below indicate that simultaneous onset generally occurs with R_1 and R_2 fairly close. We note that in the case where the upper and lower fluids are the same, (2.3) reduces to $D > 1$, i.e. we need the lower layer of fluid to be thicker than the upper layer.

We assume that the motion occurs as two-dimensional rolls. There are, of course, well-known experimental difficulties in achieving two-dimensional rolls because of the degeneracy of pattern selection at critical Rayleigh number. The analysis is considerably simpler for two-dimensional rolls than for other configurations.

Suitably scaled Navier–Stokes equations can be written in a Cartesian coordinate system with gravity in the negative z-direction and in which the velocity $\boldsymbol{u} = (-\partial\psi/\partial z,\ 0,\ \partial\psi/\partial x)$,

$$\frac{1}{p_k}\left\{C_k \frac{\partial \omega_k}{\partial t} + \frac{\partial \psi_k}{\partial x}\frac{\partial \omega_k}{\partial z} - \frac{\partial \psi_k}{\partial z}\frac{\partial \omega_k}{\partial x}\right\} = -R_k K_k \frac{\partial \theta_k}{\partial x} + \nabla^2 \omega_k, \tag{2.4}$$

$$C_k \frac{\partial \theta_k}{\partial t} + \frac{\partial \psi_k}{\partial x}\frac{\partial \theta_k}{\partial z} - \frac{\partial \psi_k}{\partial z}\frac{\partial \theta_k}{\partial x} = \frac{\partial \psi_k}{\partial x} + \nabla^2 \theta_k, \tag{2.5}$$

$$\omega_k = -\nabla^2 \psi_k. \tag{2.6}$$

Here $k = 1, 2$ refers to the equations in the two layers. $P_1 = \nu_1/\kappa_1$ and $P_2 = \nu_2/\kappa_2$ are the Prandtl numbers of the two layers, $C_1 = 1$ and $C_2 = \kappa_1/\kappa_2$, the conductivity ratio of the two fluids. R_1 and R_2 are the two Rayleigh numbers defined in (2.2) and $K_1 = 1$, $K_2 = D^4$, D being the depth ratio of the layers.

With the same scaling, the boundary conditions become

$$\theta_1 = G\theta_2, \quad C_2 \frac{\mathrm{d}\theta_1}{\mathrm{d}z} = G\frac{\mathrm{d}\theta_2}{\mathrm{d}z} \quad \text{on } z = d, \tag{2.7}$$

where $G = D^4 R_2 \kappa_2 \nu_2 \alpha_1 / R_1 \kappa_1 \nu_1 \alpha_2$.

$$\left.\begin{aligned} \theta_1 = \psi_1 = \frac{\partial \psi_1}{\partial z} = 0 \quad \text{on } z = 0, \quad \psi_1 = \frac{\partial \psi_1}{\partial z} = 0 \quad \text{on } z = d, \\ \theta_2 = \psi_2 = \frac{\partial \psi_2}{\partial z} = 0 \quad \text{on } z = d(1 + D^{-1}), \quad \psi_2 = \frac{\partial \psi_2}{\partial z} = 0 \quad \text{on } z = d. \end{aligned}\right\} \tag{2.8}$$

There are twelve boundary conditions, so the problem is of twelfth order.

The parameter G will vary considerably depending on the experimental configuration. If D is substantially greater than 1 (e.g. D close to 2 as for the 2:1 resonance) simultaneous onset in the two layers can be achieved in different ways: if the same fluid is used in both layers, the temperature gradient in the upper layer must be approximately D^4 times the gradient in the lower layer. This requires the flux F_0 to be quite close to the critical value $(T_b - T_u)\, D\kappa_2/d$, and the parameter G will also be close to D^4. Alternatively, we could use a more viscous fluid in the lower layer than in the upper layer, so that simultaneous criticality can be achieved even though the temperature gradients are comparable. In this case the flux F_0 would be comparatively small, and used to 'fine tune' to get close to the point of simultaneous onset. If the two fluids had $\alpha_1 \kappa_2 \approx \alpha_2 \kappa_1$, and viscosities such that ν_1/ν_2 was of the same order of magnitude as D^4, then we would have $G \approx 1$. So in the first case G would be of order D^4 and in the second of order 1. With $D \approx 2$ or ≈ 3 as in the strong-resonance cases, the differences are substantial, and we expect rather different nonlinear behaviour in the two cases.

3. Linear theory

The linearized form of (2.4)–(2.6) can be written

$$\nabla^6 \theta_k = R_k K_k \frac{\partial^2 \theta_k}{\partial x^2}, \quad k = 1, 2, \tag{3.1}$$

together with the boundary conditions (2.7) and (2.8). However, we can simplify the linear problem by scaling out the parameter G which occurs in the boundary conditions. We introduce $\phi_1 = \theta_1$, $\phi_2 = G\theta_2$, so that ϕ_k also satisfy

$$\nabla^6 \phi_k = R_k K_k \frac{\partial^2 \phi_k}{\partial x^2}, \quad k = 1, 2, \tag{3.2}$$

but now the boundary conditions (2.7) are replaced by

$$\phi_1 = \phi_2, \quad C_2 \frac{\mathrm{d}\phi_1}{\mathrm{d}z} = \frac{\mathrm{d}\phi_2}{\mathrm{d}z}, \tag{3.3}$$

while the boundary conditions (2.8) are not affected by the scaling. So the only parameters to come into the linear problem are R_1, R_2, D and C_2 the conductivity ratio ($K_2 = D^4$). From now on, we assume the conductivity ratio $C_2 = 1$.

We look for solutions of (3.2) of the form

$$\phi_k = f_k(z)\, \mathrm{e}^{\mathrm{i}\alpha x} \tag{3.4}$$

corresponding to two-dimensional rolls of horizontal wavenumber α. The functions $f_k(z)$ can be written

$$f_k(z) = \sum_{j=1}^{6} a_{kj} \exp(\gamma_{kj} z), \quad k = 1, 2, \tag{3.5}$$

where the a_{kj} and the γ_{kj} are 12 complex constants; the γ_{kj} are the roots of

$$(\alpha^2 + \gamma_{kj}^2)^3 = R_k K_k \alpha^2, \quad \kappa = 1, 2. \tag{3.6}$$

The a_{kj} are determined, up to an arbitrary multiplier, by the 12 boundary conditions.

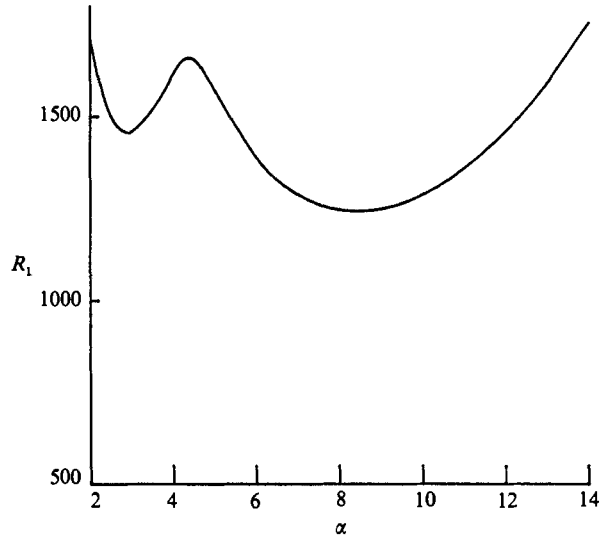

FIGURE 2. Neutral stability curve $R_1(\alpha)$ for the case $D = 3$ and $r = 1.2$.

D	r	R_1	α_1	α_2	α_2/α_1
1.5510	1.1392	1279.7	3.4105	3.6952	1.0835
1.5641	1.1360	1285.0	3.3134	3.8338	1.1571
1.6316	1.1210	1309.2	3.1237	4.2347	1.3557
1.7027	1.1078	1330.2	3.0392	4.5372	1.4929
1.8571	1.0853	1364.9	2.9570	4.9701	1.6808
2.0977	1.0607	1401.8	2.9150	5.8300	2.0000
2.1250	1.0584	1405.2	2.9128	5.9116	2.0295
2.3333	1.0436	1427.1	2.9048	6.5231	2.2456
2.7037	1.0242	1455.7	2.9074	7.5859	2.6092
3.0000	1.0126	1473.1	2.9147	8.4276	2.8914

TABLE 1. The values of r and R_1 at which simultaneous onset of two modes occurs for a range of depth ratios, D. α_1 and α_2 are the wavenumbers of the two critical modes.

If we take D and the ratio $R_2/R_1 = r$ as fixed parameters, then for any value of α we can solve the eigenvalue problem for the a_{kj} to get the eigenvalues R_1. The lowest of these gives the neutral stability curve $R_1(\alpha)$. To compute the neutral stability curve numerically, we used a routine from the Numerical Algorithm Group library to find the eigenvalues of the complex 12×12 boundary-condition matrix.

If $D > 1.55$ and r is near 1, the neutral stability curve contains not just a single minimum, but two distinct minima. In figure 2 we give an example, with $r = 1.2$, $D = 3$. This result is not unexpected, and has a simple physical interpretation. At the minimum corresponding to the larger wavenumber, the motion is predominantly in the thinner upper layer and so has a small horizontal scale comparable with the thin layer depth. At the minimum corresponding to the lower wavenumber, the convection is predominantly in the lower layer and so takes the larger horizontal scale comparable with the thicker layer depth. This argument is not precise, of

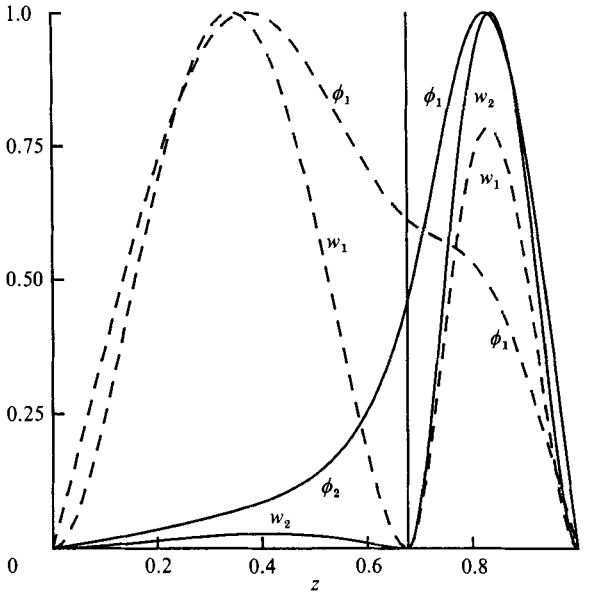

FIGURE 3. Linear eigenfunctions w and ϕ are plotted against z in the 2:1 resonance case. (All eigenfunctions are normalized to have unit maximum.)

course, because the layers are coupled through the thermal boundary conditions (this coupling is crucial in determining the nonlinear behaviour).

If we now vary r, the ratio of R_2/R_1, we can arrange to choose r so that both the minima have the same value of R_1. So with this value of r, we have a pair of values of R_1 and R_2 at which two differing convection modes onset simultaneously. Finally, by varying D, we can find a table of values of the point where the modes onset simultaneously. This is given in table 1. A number of features are apparent from this table. First, for values of $D \geqslant 2$ the ratio of the wavenumbers is not very different from the depth ratio, giving support to the physical picture given above. Second, the ratio of the Rayleigh numbers is never very different from unity again supporting the idea that at least at reasonably large D the two layers are only weakly coupled. Third, the values of R_1 and R_2 are not very different from 1708, the critical value for a single layer with fixed boundaries (Chandrasekhar 1961). Fourth, and importantly for what follows, there exists a value of D such that the two modes have wavenumbers in the ratio of 2:1. For this 2:1 resonance, the critical value of D is 2.09765.

In figure 3 we show the linear eigenfunctions for the 2:1 resonance case.

4. Weakly nonlinear theory with spatial resonance

We now return to the formulation of (2.4)–(2.6) with boundary conditions (2.7) and (2.8). We assume that the linear eigenfunctions of the two solutions which onset together are available together with the critical values of R_1 and R_2 which we denote by R_{c1} and R_{c2}. If we have solved the linear problem in terms of the variables ϕ_i satisfying (3.3), we must remember to multiply the eigenfunction in the upper layer by a factor of G^{-1}, so that boundary conditions (2.7) are satisfied (we are setting $C_2 = 1$).

It is convenient to write the equations in the form

$$\frac{1}{P_k R_{ck} K_k}\left\{\frac{\partial \omega_k}{\partial t}+\frac{\partial(\psi_k, \omega_k)}{\partial(x, z)}\right\}=\frac{R_{ck}-R_k}{R_{ck}}\frac{\partial \theta_k}{\partial x}-\frac{\partial \theta_k}{\partial x}+\frac{1}{R_{ck}K_k}\nabla^2\omega_k, \tag{4.1}$$

$$\frac{\partial \theta_k}{\partial t}+\frac{\partial(\psi_k, \theta_k)}{\partial(x, z)}=\frac{\partial \psi_k}{\partial x}+\nabla^2\theta_k, \tag{4.2}$$

$$\omega_k=-\nabla^2\psi_k, \tag{4.3}$$

where $k=1, 2$ refers to the lower and upper layer respectively.

The linear eigenfunctions can be written

$$\psi_{jk}^{(1)}=\exp(\mathrm{i}\alpha_j x)\sum_{m=1}^{6}\psi_{jkm}\exp(\gamma_{jkm}z)+\text{c.c.}, \tag{4.4}$$

$$\omega_{jk}^{(1)}=\exp(\mathrm{i}\alpha_j x)\sum_{m=1}^{6}\omega_{jkm}\exp(\gamma_{jkm}z)+\text{c.c.}, \tag{4.5}$$

$$\theta_{jk}^{(1)}=\exp(\mathrm{i}\alpha_j x)\sum_{m=1}^{6}\theta_{jkm}\exp(\gamma_{jkm}z)+\text{c.c.}, \tag{4.6}$$

where c.c. denotes complex conjugate, the index $j=1, 2$ refers to the two simultaneously onsetting modes and the index k refers to values in the two layers. For convenience, we write

$$\boldsymbol{y}_j^{(1)}\equiv(\psi_{jk}^{(1)}, \omega_{jk}^{(1)}, \theta_{jk}^{(1)}), \tag{4.7}$$

and we define

$$\boldsymbol{y}^{(1)}=A_1\boldsymbol{y}_1^{(1)}+A_2\boldsymbol{y}_2^{(1)}+\text{c.c.} \tag{4.8}$$

where the amplitudes A_j are complex and are slowly varying functions of time. We consider the effect of slow spatial variation in a later paper.

We must now distinguish between spatially resonant cases, where α_1 and α_2 satisfy a relation of the form

$$n\alpha_1+m\alpha_2=0, \quad n, m \text{ integers} \tag{4.9}$$

and cases where the wavenumbers are non-resonant. In this problem it appears that the most interesting cases are the strong resonances where the wavenumbers α_2 and α_1 are in a 2:1 or a 3:1 ratio. When resonances are present extra terms enter the amplitude equations which are absent when there is no resonance. In the case of 2:1 resonance these new terms enter at second order, but we must retain third-order terms to determine the amplitudes A_1 and A_2. In the 3:1 resonance the new terms are third order. Since in these cases the resonances make an $O(1)$ change in the amplitudes near onset, we call these strong resonances (see also Coullet 1986).

4.1. *Non-resonant wavenumbers*

The appropriate scalings for the non-resonant case are

$$\boldsymbol{y}=\epsilon(A_1\boldsymbol{y}_1^{(1)}+A_2\boldsymbol{y}_2^{(1)})+\epsilon^2\boldsymbol{y}^{(2)}+\epsilon^3\boldsymbol{y}^{(3)}, \tag{4.10}$$

with the slow timescale $\tilde{t}=\epsilon^2 t$ and

$$\frac{R_k-R_{ck}}{R_{ck}}=\epsilon^2 R_{2k}, \quad k=1, 2. \tag{4.11}$$

$O(\epsilon^2)$-terms are generated by inserting the linear $O(\epsilon)$-eigenfunctions into the quadratic Jacobian terms in (4.1) and (4.2). This leads to an inhomogeneous linear problem for $\boldsymbol{y}_2^{(2)}$,

$$L\boldsymbol{y}^{(2)} = M(\boldsymbol{y}^{(1)}, \boldsymbol{y}^{(1)}), \tag{4.12}$$

where the terms in M have the form

$$A_1^2\,\mathrm{e}^{2\mathrm{i}\alpha_1 x} f_1 + A_2^2\,\mathrm{e}^{2\mathrm{i}\alpha_2 x} f_2 + A_1 A_2\,\mathrm{e}^{\mathrm{i}(\alpha_1+\alpha_2)x} f_3 + A_2 \bar{A}_1\,\mathrm{e}^{\mathrm{i}(\alpha_2-\alpha_1)x} f_4 + A_1 \bar{A}_1 f_5 + A_2 \bar{A}_2 f_6 + \text{c.c.}, \tag{4.13}$$

the f_i being functions of z. The functions $f_i(z)$ can be written as double sums of exponentials, e.g.

$$f_1 = \sum_{m=1}^{6} \sum_{n=1}^{6} a_{1kmn} \exp(\gamma_{1km} + \gamma_{1kn}) z \tag{4.14}$$

where the index k refers as before to the two layers. Equation (4.12) can be solved straightforwardly, so that we can proceed to the $O(\epsilon^3)$-terms. The Jacobians now give terms arising from combining $\boldsymbol{y}^{(1)}$ and $\boldsymbol{y}^{(2)}$, so we get terms proportional to $\mathrm{e}^{\mathrm{i}\alpha_1 x}$ and $\mathrm{e}^{\mathrm{i}\alpha_2 x}$. Because $\alpha_{1,2}$ do not satisfy (4.5), the only such terms have the form

$$(A_1|A_1|^2 g_1 + A_1|A_2|^2 g_2)\,\mathrm{e}^{\mathrm{i}\alpha_1 x} + (A_2|A_2|^2 g_3 + A_2|A_1|^2 g_4)\,\mathrm{e}^{\mathrm{i}\alpha_2 x} + \text{c.c.} \tag{4.15}$$

The time-dependent terms and the departure of R_i from their critical values also enter at the $O(\epsilon^3)$-level. To derive the amplitude equations, we need to derive the adjoint eigenfunctions from the inner product which is

$$\int_0^1 \psi^\dagger \left(\frac{1}{R_1 K1}\nabla^2\omega - \frac{\partial\theta}{\partial x}\right) + \theta^\dagger\left(\nabla^2\theta + \frac{\partial\psi}{\partial x}\right) \mathrm{d}z + G^2 \int_1^{(1+D^{-1})} \psi^\dagger \left(\frac{1}{R_2 K_2}\nabla^2\omega - \frac{\partial\theta}{\partial x}\right) + \theta^\dagger\left(\nabla^2\theta + \frac{\partial\psi}{\partial x}\right) \mathrm{d}z = \langle \boldsymbol{y}^{(1)}, \boldsymbol{y}^{(1)\dagger}\rangle. \tag{4.16}$$

Integration by parts, using the boundary conditions (2.7) and (2.8) together with the same boundary conditions applied to $\psi^\dagger$ and $\theta^\dagger$, shows that the problem is self-adjoint; that is the adjoint $(\psi^\dagger, \omega^\dagger, \theta^\dagger)$ satisfies the same problem as (ψ, ω, θ), and so we can take the adjoint eigenfunctions as equal to the original ones. This procedure leads to amplitude equations of the form

$$\left.\begin{aligned} \dot{A}_1 &= \mu_1 A_1 - a_1 A_1|A_1|^2 - b_1 A_1|A_2|^2, \\ \dot{A}_2 &= \mu_2 A_2 - a_2 A_2|A_2|^2 - b_2 A_2|A_1|^2, \end{aligned}\right\} \tag{4.17}$$

where $\mu_1 = c_{11}R_{21} + c_{12}R_{22}$ and $\mu_2 = c_{21}R_{21} + c_{22}R_{22}$, where terms generated by the expansion up to $O(\epsilon^3)$ have been included. Equations of this type have been derived in a number of different physical contexts.

4.2. *The* 2:1 *resonance*

We now consider the case where $\alpha_2 = 2\alpha_1 = 2\alpha$, a circumstance which occurs in our problem when $D = 2.098$. Coefficients in a 2:1 resonance situation have been previously computed by Rosenblat, Davis & Homsy (1982) in connection with Marangoni convection, but our technique is slightly different.

We again adopt an expansion of the type (4.10), but now the slow timescale is $\tilde{t} = \epsilon t$ and we write

$$\frac{R_k - R_{ck}}{R_{ck}} = \epsilon R_{2k}, \quad k = 1, 2, \tag{4.18}$$

in contrast to (4.11). When the linear eigenfunctions are inserted into the nonlinear Jacobian terms in (4.1) and (4.2), terms of the type

$$M_2^{(2)} \equiv A_2^2 \,\mathrm{e}^{4\mathrm{i}\alpha x} f_1 + A_1 A_2 \,\mathrm{e}^{3\mathrm{i}\alpha x} f_2 + A_1^2 \,\mathrm{e}^{2\mathrm{i}\alpha x} f_3 + A_2 \bar{A}_1 \,\mathrm{e}^{\mathrm{i}\alpha x} f_4 + A_1 \bar{A}_1 f_5 + A_2 \bar{A}_2 f_6 + \text{c.c.} \tag{4.19}$$

are generated. In fact that terms proportional to $\mathrm{e}^{\mathrm{i}\alpha x}$, $\mathrm{e}^{2\mathrm{i}\alpha x}$ are present means that it is not possible to solve for $\psi^{(2)}$ without bringing in the terms involving $(R_i - R_{ci})/R_{ci}$. This is why (4.18) differs from (4.11), and why the timescale is $O(\epsilon)$. The coefficients of the second-order amplitude equation can be determined in the usual way, by multiplying through by the adjoint and integrating: the exact form of the integral is dictated by the form of (4.16). The resulting amplitude equations have the form

$$\left.\begin{aligned} \dot{A}_1 &= \mu_1 A_1 + \mathrm{i}\alpha_0 A_2 \bar{A}_1, \quad \dot{A}_2 = \mu_2 A_2 + \mathrm{i}\alpha_0 A_1^2, \\ \mu_1 &= c_{11} R_{21} + c_{12} R_{22}, \quad \mu_2 = c_{21} R_{21} + c_{22} R_{22}, \end{aligned}\right\} \tag{4.20}$$

where α_0 is real. The fact that the same coefficient appears in front of the nonlinear terms is due to the normalization of the eigenfunctions: this was chosen so that

$$\langle \boldsymbol{y}_1^{(1)}, \boldsymbol{y}_1^{(1)\dagger} \rangle = \langle \boldsymbol{y}_2^{(1)}, \boldsymbol{y}_2^{(1)\dagger} \rangle = 1. \tag{4.21}$$

It would be consistent to stop at $O(\epsilon^2)$ with (4.20), but the quadratic terms in (4.20) have an energy-preserving character and do not determine finite amplitudes: from (4.20) it follows that

$$\frac{\mathrm{d}}{\mathrm{d}t}\left[|A_1|^2 + |A_2|^2\right] = \mu_1 |A_1|^2 + \mu_2 |A_2|^2 \tag{4.22}$$

so that if, for example, both μ_1 and μ_2 are positive (both modes supercritical) (4.20) predicts that the amplitudes tend to infinity. We must therefore go on to introduce the cubic $O(\epsilon^3)$-terms, even though these are formally $O(\epsilon)$ compared to the quadratic terms.

For consistency, we derive all the $O(\epsilon)$-terms, although as we shall see some can be absorbed by renormalization. To do this we have to compute $\boldsymbol{y}^{(2)}$, the second-order solutions, explicitly. The second-order problem has the form of inhomogeneous linear equations

$$L\boldsymbol{y}^{(2)} = M_{\mathrm{R}}^{(2)}(\boldsymbol{y}^{(1)}, \boldsymbol{y}^{(1)}) + M_{\mathrm{N}}^{(2)}(\boldsymbol{y}^{(1)}, \boldsymbol{y}^{(1)}) + N^{(2)}(\boldsymbol{y}^{(1)}), \tag{4.23}$$

where $M_{\mathrm{R}}^{(2)}$ is the resonant part of the Jacobian having terms of the form

$$A_1^2 \,\mathrm{e}^{2\mathrm{i}\alpha x} f_3(z) + A_2 \bar{A}_1 \,\mathrm{e}^{\mathrm{i}\alpha x} f_4(z) + \text{c.c.} \tag{4.24}$$

$M_{\mathrm{N}}^{(2)}$ is the non-resonant part of the Jacobian having terms of the form

$$A_2^2 \,\mathrm{e}^{4\mathrm{i}\alpha x} f_1(z) + A_1 A_2 \,\mathrm{e}^{3\mathrm{i}\alpha x} f_2(z) + A_1 \bar{A}_1 f_5(z) + A_2 \bar{A}_2 f_6(z) + \text{c.c.}, \tag{4.25}$$

and $N^{(2)}$ are the terms coming from the time derivatives and the terms proportional to R_{2i}, so they have the form

$$(\dot{A}_1 g_1 + A_1 R_{21} g_2 + A_1 R_{22} g_3) \,\mathrm{e}^{\mathrm{i}\alpha x} + (\dot{A}_2 g_4 + A_2 R_{21} g_5 + A_2 R_{23} g_6) \,\mathrm{e}^{2\mathrm{i}\alpha x} + \text{c.c.} \tag{4.26}$$

As before, the non-resonant terms give no difficulty, but the resonant terms need special treatment.

The method of solution is to find a particular integral for these terms, which is straightforward, and then to add on terms of the form

$$b_{km} \exp(\mathrm{i}\alpha_j x) \exp(\gamma_{jkm} z) \tag{4.27}$$

to satisfy the boundary conditions. For each j there are 12 b_{km} coefficients, since $k = 1, 2$ and $m = 1, \ldots, 6$. However, although the 12 boundary conditions give rise to a matrix equation

$$\boldsymbol{B}\boldsymbol{b} = \boldsymbol{r}, \tag{4.28}$$

the matrix $\boldsymbol{B}$ is singular, of rank 11, because R_{ci} are eigenvalues. We set $b_{12} = 1$ and solve the 11×11 system formed by omitting the last equation: the last equation then gives a relation which is just the amplitude equation. The procedure is repeated for $j = 1$ and 2, giving a useful numerical check on the coefficients in (4.20). This is particularly helpful as without a fully two-dimensional calculation there are not many checks available on the numerical values of the coefficients of the amplitude equations.

Now that the boundary conditions are satisfied, the last step in the calculation of $\boldsymbol{y}^{(2)}$ is to add on a suitable multiple of $\boldsymbol{y}^{(1)}$ so that the normalization condition

$$\langle \boldsymbol{y}_1^{(2)}, \boldsymbol{y}_1^{(1)\dagger} \rangle = \langle \boldsymbol{y}_2^{(2)}, \boldsymbol{y}_2^{(1)\dagger} \rangle = 0 \tag{4.29}$$

is satisfied.

We now do the $O(\epsilon^3)$-terms; the Jacobians give terms arising from products of $\boldsymbol{y}^{(1)}$ and $\boldsymbol{y}^{(2)}$. We might expect terms of the form $\ddot{A}_j$ to arise at this order, but in fact the coefficient associated with such terms is zero. The coefficients of the amplitude equations are found by multiplying through by the adjoint and integrating as usual.

We obtain the following terms with non-zero coefficients:

$$\left.\begin{aligned} \tilde{f}_1 \dot{A}_1 &= \tilde{\mu}_1 A_1 + \mathrm{i}\tilde{\alpha}_1 A_2 \bar{A}_1 - \epsilon\{\tilde{a}_1 A_1 |A_1|^2 + \tilde{b}_1 A_1 |A_2|^2 + \mathrm{i}\tilde{d}_1 \dot{A}_2 \bar{A}_1 + \mathrm{i}\tilde{e}_1 A_2 \dot{\bar{A}}_1\}, \\ \tilde{f}_2 \dot{A}_2 &= \tilde{\mu}_2 A_2 + \mathrm{i}\tilde{\alpha}_2 A_1^2 - \epsilon\{\tilde{a}_2 A_2 |A_2|^2 + \tilde{b}_2 A_2 |A_1|^2 + \mathrm{i}\tilde{d}_2 \dot{A}_1 A_1\}, \end{aligned}\right\} \tag{4.30}$$

where

$$\left.\begin{aligned} \tilde{\mu}_j &= c_{j1} R_{21} + c_{j2} R_{22} + \epsilon\{\tilde{c}_{j11} R_{21}^2 + \tilde{c}_{j12} R_{21} R_{22} + \tilde{c}_{j22} R_{22}^2\}, \\ \tilde{\alpha}_j &= \alpha_0 + \epsilon(\tilde{\alpha}_{j1} R_{21} + \tilde{\alpha}_{j2} R_{22}), \\ \tilde{f}_j &= 1 + \epsilon(\tilde{f}_{j1} R_{21} + \tilde{f}_{j2} R_{22}). \end{aligned}\right\} \tag{4.31}$$

The terms $\mathrm{i}\tilde{d}_1 \dot{A}_2 \bar{A}_1$, $\mathrm{i}\tilde{d}_2 \dot{A}_1 A_1$ and $\mathrm{i}\tilde{e}_1 A_2 \dot{\bar{A}}_1$ can be eliminated using the second-order equations (4.20). We then divide through each equation by $\tilde{f}_1$ and $\tilde{f}_2$ and finally rescale A_2 so that the coefficient in front of the $A_2 \bar{A}_1$ is the same as that in front of the A_1^2 term. We then have

$$\left.\begin{aligned} \dot{A}_1 &= \mu_1 A_1 + \mathrm{i}\alpha A_2 \bar{A}_1 - \epsilon\{a_1 A_1 |A_1|^2 + b_1 A_1 |A_2|^2\}, \\ \dot{A}_2 &= \mu_2 A_2 + \mathrm{i}\alpha A_1^2 - \epsilon\{a_2 A_2 |A_2|^2 + b_2 A_2 |A_1|^2\}, \end{aligned}\right\} \tag{4.32}$$

where

$$\left.\begin{aligned} \mu_j &= c_{j1} R_{21} + c_{j2} R_{22} + \epsilon\{c_{j11} R_{21}^2 + c_{j12} R_{21} R_{22} + c_{j22} R_{22}^2\}, \\ \alpha &= \alpha_0 + \epsilon\{\alpha_1 R_{21} + \alpha_2 R_{22}\}, \end{aligned}\right\} \tag{4.33}$$

and the coefficients appearing in (4.33) can be easily evaluated in terms of those appearing in (4.31).

The coefficients in (4.32) will depend on the Prandtl numbers and the parameter G, assuming the two fluids have the same thermal diffusivity. The parameter G depends on how the experiment is performed, as explained in §2. In table 2 we give the coefficients for $G = D^4 R_2 / R_1 = 20.537$, the one-fluid case, and with $P_1 = P_2 = 0.1$, 1.0, 10 and 100. We also give the results for $G = 1$, $P_2 = 0.1$, 1.0, 10 and 100 and $P_1 = 20.537 P_2$.

	$G = 20.54$ $P = 0.1$	$G = 20.54$ $P = 1.0$	$G = 20.54$ $P = 10.0$	$G = 20.54$ $P = 100.0$	$G = 1.0$ $P = 0.1$	$G = 1.0$ $P = 1.0$	$G = 1.0$ $P = 10.0$	$G = 1.0$ $P = 100.0$
α_0	1.504	3.700	4.354	4.434	8.295	11.903	13.147	13.304
α_1	−6.230	−9.536	−10.579	−10.710	36.091	46.049	49.310	49.731
α_2	−177.01	−166.07	−163.30	−162.93	115.18	226.71	268.90	274.47
c_{11}	9.077	11.264	11.542	11.570	10.193	11.419	11.558	11.572
c_{12}	1.773	2.201	2.255	2.260	1.991	2.231	2.258	2.261
a_1	120.58	219.88	235.34	236.98	281.73	309.86	317.51	318.42
b_1	−2.061	−12.152	−16.286	−16.836	717.03	1309.8	1707.4	1762.2
c_{111}	14.320	15.279	15.465	15.485	17.821	15.644	15.502	15.489
c_{112}	−5.972	−5.188	−4.975	−4.951	−7.068	−5.285	−4.984	−4.952
c_{122}	1.543	2.411	2.540	2.553	1.573	2.429	2.542	2.554
c_{21}	0.085	0.280	0.363	0.374	0.085	0.280	0.363	0.374
c_{22}	12.979	42.625	55.244	56.929	12.987	42.634	55.245	56.930
a_2	38.369	23.011	3.600	41.009	1474.3	10282.3	17246.0	18321.2
b_2	−4.493	−17.238	−22.736	−23.471	−46.234	−79.404	−145.47	−154.43
c_{211}	0.058	0.183	0.235	0.241	0.058	0.184	0.235	0.241
c_{212}	−0.094	−1.236	−1.972	−2.076	−0.074	−1.214	−1.968	−2.076
c_{222}	−2.018	−4.019	−6.971	−9.361	−2.029	−4.062	−6.963	−9.360
Δ	472.6	843.7	901.9	908.3	4127.8	13983	21640	22810

TABLE 2. The coefficients of the amplitude equations (4.32) and (4.33) for various Prandtl numbers. $G = 20.537$ is the one-fluid model, $G = 1$ the two-fluid model.

5. Analysis of the evolution equations in the case of 2:1 resonance

5.1. *Reduction of order*

We begin with (4.32) derived in the previous section, namely

$$\left.\begin{aligned} \dot{A}_1 &= \mu_1 A_1 + \mathrm{i}\alpha A_2 \bar{A}_1 - a_1 A_1 |A_1|^2 - b_1 A_1 |A_2|^2, \\ \dot{A}_2 &= \mu_2 A_2 + \mathrm{i}\alpha A_1^2 - b_2 A_2 |A_1|^2 - a_2 A_2 |A_2|^2, \end{aligned}\right\} \tag{5.1a,b}$$

where the terms in ϵ have been rescaled, as can be done since the dynamics are scale invariant. These equations have been analysed in some detail by Dangelmayr & Armbruster (1986; see also Dangelmayr 1986), who in fact treated all important $m:n$ resonances. A similar set of equations (with the μ_i, a_i, b_i complex) appears in the normal form for two interacting Hopf bifurcations with frequencies in the ratio 2:1. A partial analysis is given by Knobloch & Proctor (1988). Here we summarize their main results, and add new ones of our own. In particular, while we essentially reproduce the above authors' results for steady solutions and travelling-wave solutions, we are able to give, in a certain portion of parameter space, a more or less complete discussion of the branch of modulated waves that appear and determine its stability. We also give a discussion of an attracting homoclinic orbit that appears in a surprisingly large region of parameter space, and show how this rather unphysical behaviour may be resolved by including extra terms in (5.1) representing imperfections in the system.

We begin by using the translational invariance of our original problem to reduce the order of (5.1), writing

$$A_1 = \rho\, \mathrm{e}^{\mathrm{i}\theta}, \quad A_2 = \sigma\, \mathrm{e}^{\mathrm{i}\phi} \tag{5.2}$$

Substituting and equating real and imaginary parts, we obtain

$$\dot{\rho} = \mu_1 \rho + \alpha\rho\sigma \cos\chi - a_1 \rho^3 - b_1 \rho\sigma^2, \tag{5.3a}$$

$$\rho\dot{\theta} = -\alpha\rho\sigma \sin\chi, \tag{5.3b}$$

$$\dot{\sigma} = \mu_2 \sigma - \alpha\rho^2 \cos\chi - b_2 \rho^2 \sigma - a_2 \sigma^3, \tag{5.3c}$$

$$\sigma\dot{\phi} = -\alpha\rho^2 \sin\chi, \tag{5.3d}$$

where $\chi = 2\theta - \phi - \frac{1}{2}\pi$, and (5.3*b*, *d*) may be combined to give

$$\dot{\chi} = \alpha\left(\frac{\rho^2}{\sigma} - 2\sigma\right)\sin\chi. \tag{5.4}$$

Thus the system is reduced to third order (this is clearly possible since the origin in x is arbitrary). Once ρ, σ and χ are found θ and ϕ may be determined from (5.3*b*, *d*). We shall investigate this third-order system for general values of a_1, b_1, a_2, b_2 though bearing in mind in our selection of examples the values given for the experiment described earlier. The results are best represented as bifurcation diagrams in the (μ_1, μ_2)-plane: two typical cases are shown as figures 4 and 5.

Solutions of constant amplitude

We now seek solutions such that $\dot{\rho} = \dot{\sigma} = \dot{\chi} = 0$. These fall into three types.

(i) Pure modes (P_+, P_-):

$$\rho = 0, \quad \sigma^2 = \frac{\mu_2}{a_2}, \quad \chi_+ = 0, \quad \chi_- = \pi. \tag{5.5}$$

These modes exist if $a_2\mu_2 > 0$ and represent steady convection with period 1. Strictly the value of χ is irrelevant when $\rho = 0$ but the labelling will prove useful later.

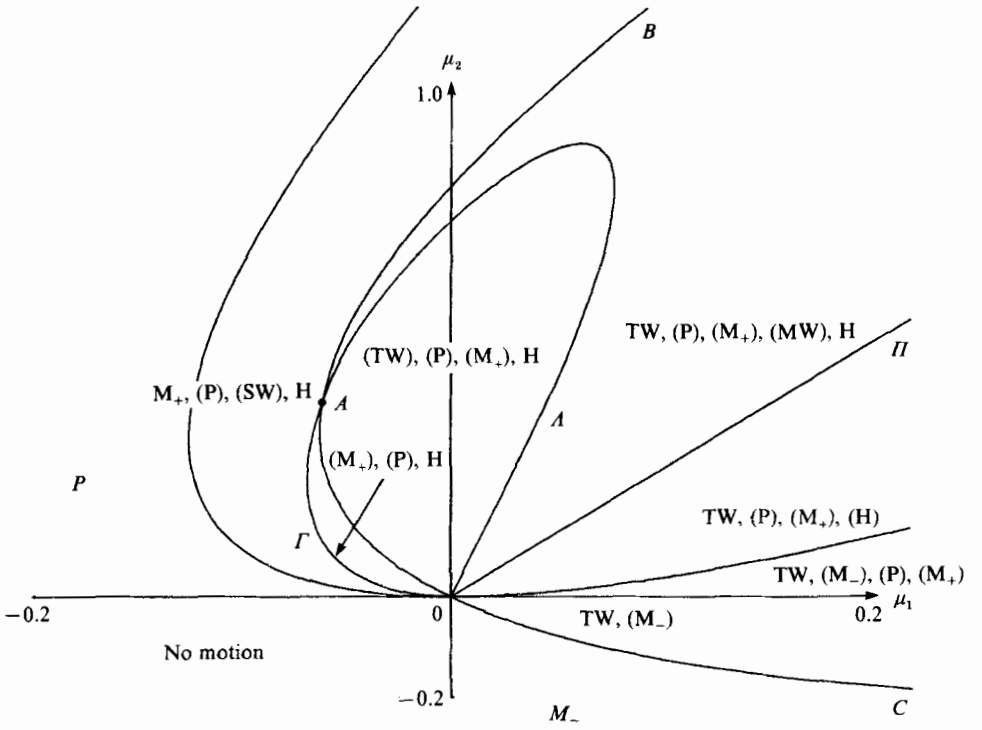

FIGURE 4. Bifurcation diagram for a case ($\alpha = 1$, $a_1 = 1$, $b_1 = 2$, $a_2 = 5$, $b_2 = 0$) in which the branch of modulated waves is unstable. Travelling waves exist to the right of the parabola $COAB$ and are stable to the right of curve Λ. Stable and unstable solutions are given in each region, the latter bracketed. The line Γ is the Hopf bifurcation of the state M_+, Λ the Hopf bifurcation of the travelling-wave branch and Π the homoclinic orbit for the modulated waves, and the line on which the structurally stable homoclinic orbit ceases to be attracting.

(ii) Mixed modes ($M_\pm$):

$$\left.\begin{aligned} 0 &= \mu_1 \pm \alpha\sigma - a_1\rho^2 - b_1\sigma^2, \\ 0 &= \mu_2\sigma \mp \alpha\rho^2 - b_2\rho^2\sigma - a_2\sigma^3, \\ \chi_+ &= 0, \quad \chi_- = \pi \end{aligned}\right\} \tag{5.6}$$

These solutions represent steady convection with period 2. The two modes are quite distinct, and have very different stability properties.

(iii) Travelling waves (TW):

$$\left.\begin{aligned} \rho^2 = 2\sigma^2; \quad \sigma^2 &= \frac{2\mu_1+\mu_2}{\Delta}; \quad \Delta \equiv 4a_1 + 2(b_1+b_2) + a_2, \\ \cos\chi &= \frac{1}{\alpha\sigma}\frac{\mu_2(2a_1+b_1) - \mu_1(2b_2+a_2)}{\Delta}. \end{aligned}\right\} \tag{5.7}$$

There are two of these waves, one travelling in each direction, but we shall not distinguish them. They exist provided $(2\mu_1+\mu_2)\Delta > 0$ and $|\cos\chi| \leqslant 1$, i.e. when

$$[(2a_1+b_1)\mu_2 - (2b_2+a_2)\mu_1]^2 \leqslant \alpha^2(2\mu_1+\mu_2)\Delta. \tag{5.8}$$

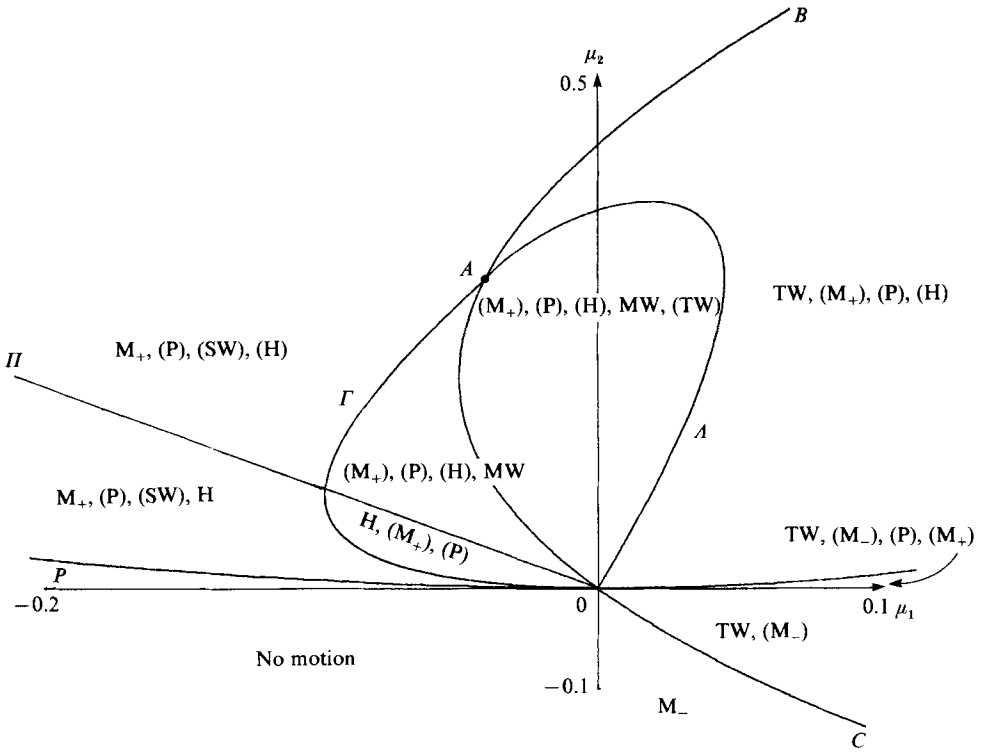

FIGURE 5. As figure 4, but for a case in which the modulated waves are stable: $\alpha = 1$, $a_1 = 3$, $b_1 = 1$, $a_2 = 1$, $b_2 = 0$.

The phase speed of the waves is given by $-2\alpha\sigma \sin\chi$. It follows that when equality holds in (5.8) the phase speed vanishes, so that the travelling waves bifurcate there from one or other of the M-modes. The latter modes themselves bifurcate from the pure-mode solution on the lines

$$0 = \mu_1 - \frac{b_1\mu_2}{a_2} \pm \alpha\left(\frac{\mu_2}{a_2}\right)^{\frac{1}{2}}. \tag{5.9}$$

It should be noted that the time dependence of these solutions arises solely from the nonlinear interaction of the competing modes (in particular, the phase speed goes to zero at the codimension-2 point). Thus this behaviour is somewhat different from the codimension-2 bifurcation arising at the double Hopf bifurcation with $O(2)$ symmetry occurring in binary fluids (see e.g. Kolodner *et al.* 1986). The stability of these relatively simple solutions may be found by standard methods. In view of the work of Dangelmayr & Armbruster (1986) we do not give here an exhaustive list of possible cases, but concentrate on the particular case $a_1 > 0$, $a_2 > 0$, $\Delta > 0$ that holds in our experiment. Then for $\mu_1, \mu_2 < 0$ there is no motion, while for $\mu_2 > 0$ the pure mode is stable for

$$\mu_1 < \frac{b_1\mu_2}{a_2} - \alpha\left(\frac{\mu_2}{a_2}\right)^{\frac{1}{2}}.$$

For μ_1 just greater than this value the stable solution is the mixed mode M_+ given by (5.6). The latter mode in turn loses stability at a Hopf bifurcation as μ_1 is further increased. This bifurcation, which does not involve the phase χ may be located by

standard methods, and lies on the line in (μ_1, μ_2)-space given by (5.6) together with

$$2a_1\rho^2 + 2a_2\sigma^2 = \frac{\alpha\rho^2}{\sigma}. \tag{5.10}$$

The relation between μ_1 and μ_2 cannot be written in closed form, but for small μ_1, μ_2, ρ, σ it is given approximately by

$$\mu_1 \sim -\alpha\sigma \sim -\alpha\left(\frac{\mu_2}{3a_2}\right)^{\frac{1}{2}}, \quad \rho \sim \left(\frac{2a_2\sigma^3}{\alpha}\right)^{\frac{1}{2}}. \tag{5.11}$$

Strictly speaking the condition (5.10) is that for the existence of two equal and opposite eigenvalues to the perturbation equations to M_+; for the eigenvalues to be complex conjugate there is the extra condition that the amplitudes ρ, σ satisfy

$$a_1\left(2a_2\sigma^2 - \frac{\alpha\rho^2}{\sigma}\right) + (\alpha - 2b_1\sigma)(b_2\sigma + \alpha) \geqslant 0. \tag{5.12}$$

It is easily seen that this relation is satisfied for sufficiently small ρ, σ, since from (5.11) $\rho^2/\sigma \ll 1$ in that case. The Hopf bifurcation that occurs appears to be subcritical in the regime of interest, and leads to growing oscillations in amplitude (but not in phase). These *standing waves* grow until they lose stability with respect to phase; they then approach an attracting homoclinic trajectory, leading to a solution for which ρ is non-zero only in pulses that are separated by intervals of ever longer duration. We discuss these waves below (§6).

The other mixed-mode branch (M_-) does not suffer a Hopf bifurcation. This can be seen by noting that the necessary condition for such a singularity is (5.10) with α replaced by $-\alpha$.

The line of Hopf bifurcations eventually meets the boundary of the region given by (5.8). Here $\rho^2 = 2\sigma^2$, so substituting into (5.10) we obtain

$$\rho^2 = 2\sigma^2 = \frac{2\alpha^2}{(2a_1 + a_2)^2} \tag{5.13}$$

and μ_1 and μ_2 can then be found from (5.7), (5.8). This interesting point (labelled A in figures 4 and 5) is one for which the linearized stability problem for the steady solutions has all three eigenvalues with zero real part (one real, two complex conjugate). It is of course necessary that (5.12) be satisfied when (5.13) holds; this will occur if

$$2(a_1a_2 - b_1b_2) + (2a_1 + a_2)(a_2 + b_2 - 2b_1) \geqslant 0. \tag{5.14}$$

Plainly values of the a_i, b_i can be found (even with $a_1a_2 > b_1b_2$, $\Delta > 0$) for which (5.14) is not satisfied. In that case the line of Hopf bifurcations does not meet the line given by (5.8) but instead ends in a fold catastrophe. The dynamics in this case is not understood completely, but fortunately (5.14) is satisfied for the values of a_i, b_i obtaining in the particular problem studied in this paper. We therefore make the case where (5.14) is not satisfied the subject of future work.

The travelling waves given by (5.7) may also be stable or unstable, depending on the values of μ_1, μ_2. If, again, we suppose that (5.14) holds, there is in fact a line of Hopf bifurcations connecting the origin O and the point A. This line is given parametrically by (5.7) together with the relation

$$\begin{aligned}(2a_2\sigma^2 + 4a_1\sigma^2 - 2\alpha\sigma\cos\chi)\,[4a_1\sigma^2(2a_2\sigma^2 - 2\alpha\sigma\cos\chi) \\ + (2\alpha\sigma\cos\chi + 2b_2\sigma^2)(2\alpha\sigma\cos\chi - 4b_1\sigma^2) + 12\alpha^2\sigma^2\sin^2\chi] = 8\alpha^2\Delta\sigma^4\sin^2\chi\end{aligned} \tag{5.15}$$

and is shown on the figures as the curve Γ. The solutions that bifurcate from the travelling waves on Γ are *modulated waves*, for which both the amplitude and phase of A_1 and A_2 change in time. Close to Γ, at least, the modulations are strictly periodic, since they correspond to a periodic solution of the third-order system (5.3). Their nature can most easily be comprehended close to the origin, and in §6 below we give a full analysis in that case, showing under what conditions they are stable. We end this section by noting that in many cases travelling waves are *stable* for all (μ_1, μ_2) within the parabola given by (5.8) and to the right of Γ. They can thus be seen as an important phenomenon whenever two resonant modes interact close to the onset of instability. Even for the most exotic combination of the coefficients a_i, b_i there is always a region of the (μ_1, μ_2)-plane for which travelling waves are stable.

6. Bifurcations from the steady solutions

6.1. *Stability of travelling waves at large amplitude*

In this section we consider bifurcations from solutions discussed in §5. We begin with the travelling waves, and treat first of all the simplest problem, that of analysing their stability far from the origin (or, alternatively, for small values of α: the two conditions are equivalent under a scaling of the amplitudes ρ, σ and of the μ_i). It is convenient to regard α as a small parameter. This means that travelling waves, as well as having to satisfy the exact relation $\rho^2 = 2\sigma^2$, must also satisfy the approximate equations

$$\left.\begin{aligned} \mu_1 &= a_1\rho^2 + b_1\sigma^2, \\ \mu_2 &= a_2\sigma^2 + b_2\rho^2. \end{aligned}\right\} \tag{6.1}$$

Thus the waves only exist in the neighbourhood of the line

$$\mu_2 = \lambda_0\mu_1; \quad \lambda_0 = \frac{a_2+2b_2}{2a_1+b_1}. \tag{6.2}$$

We then keep μ_1 fixed, and write

$$\left.\begin{aligned} \mu_2 = \lambda\mu_1, \quad \lambda = \lambda_0+\alpha\lambda_1, \\ \rho = \rho_0+\alpha\rho_1, \quad \sigma = \sigma_0+\alpha\sigma_1; \quad \rho_0^2 = 2\sigma_0^2 = \frac{2\mu_1}{2a_1+b_1}. \end{aligned}\right\} \tag{6.3}$$

It is plain from (5.4) that the phase χ will then adjust on the very slow timescale $T_2 = \alpha^2 t$ to changes in ρ and σ, which themselves will adjust on the timescale t during which χ may be regarded as a constant. The evolution equation on the t timescale is then, correct to $O(\alpha)$,

$$\left.\begin{aligned} \frac{\mathrm{d}\rho_1}{\mathrm{d}t} &= \rho_0\sigma_0\cos\chi - 2a_1\rho_0^2\rho_1 - 2b_1\rho_0\sigma_0\sigma_1, \\ \frac{\mathrm{d}\sigma_1}{\mathrm{d}t} &= -\rho_0^2\cos\chi + \lambda_1\mu_1\sigma_0 - 2a_2\sigma_0^2\sigma_1 - 2b_2\rho_0\sigma_0\rho_1 \end{aligned}\right\} \tag{6.4}$$

and provided $a_1a_2 > b_1b_2$ and $2a_1+a_2 > 0$, ρ_1 and σ_1 will tend to values given by setting the right-hand sides equal to zero. Solving for ρ_1, σ_1 we obtain

$$\left.\begin{aligned} \rho_1 &= P\cos\chi + Q\lambda_1, \\ \sigma_1 &= R\cos\chi + S\lambda_1, \end{aligned}\right\} \tag{6.5}$$

where
$$\left.\begin{aligned} P &= \frac{\sqrt{2}(a_2+2b_1)}{4D}, \quad Q = -\frac{\sqrt{2}b_1\mu_1}{4\sigma_0 D}, \\ R &= -\frac{(b_2+2a_1)}{2D}, \quad S = \frac{2a_1\mu_1}{4\sigma_0 D} \end{aligned}\right\} \tag{6.6}$$

and
$$D = a_1a_2 - b_1b_2.$$

Then the equation for the evolution of χ on the timescale T_2 is

$$\begin{aligned} \frac{\mathrm{d}\chi}{\mathrm{d}T_2} &= \left[\frac{2\rho_0}{\sigma_0}\rho_1 - \frac{\rho_0^2}{\sigma_0^2}\sigma_1 - 2\sigma_1\right]\sin\chi \\ &= (W\cos\chi + U\lambda_1)\sin\chi, \end{aligned} \tag{6.7}$$

where
$$W = 2\sqrt{2P-4R} = \frac{\Delta}{D}, \quad U = 2\sqrt{2Q-4S}. \tag{6.7}$$

If we write $C = \cos\chi$, then (6.7) becomes

$$\frac{\mathrm{d}C}{\mathrm{d}T_2} = -(1-C^2)(WC+U\lambda_1) \quad (C^2 < 1). \tag{6.8}$$

This has fixed points at $C = \pm 1$, and at $C = -U\lambda_1/W$. Clearly the latter is stable if $W > 0$. Thus, as noted in §5, travelling waves are stable everywhere for small α (or large amplitude) provided $\Delta > 0$, $D > 0$ and $2a_1 + a_2 > 0$.

6.2. *Modulated-wave solutions at small amplitude*

Typically the bifurcation of the modulated waves from the travelling waves involves dynamics that are fully three-dimensional except in the neighbourhood of the bifurcation point. However, the entire structure of the modulated waves branch can be investigated when μ_1 and μ_2 are both small (or equivalently if α is large). If in (5.1) we set

$$\frac{\partial}{\partial t} = \epsilon\frac{\partial}{\partial \tilde{t}}, \quad A_i = \epsilon\tilde{A}_i, \quad \mu_i = \epsilon^2\tilde{\mu}_i, \quad i = 1, 2; \quad \epsilon \ll 1. \tag{6.9}$$

then substituting in and dropping the tilde's, we obtain

$$\left.\begin{aligned} \dot{A}_1 &= \mathrm{i}\alpha A_2\bar{A}_1 + \epsilon[\mu_1 - a_1|A_1|^2 - b_1|A_2|^2A_1], \\ \dot{A}_2 &= \mathrm{i}\alpha A_1^2 + \epsilon[\mu_2 - a_2|A_2|^2 - b_2|A_1|^2A_2]. \end{aligned}\right\} \tag{6.10}$$

If we now ignore the terms in ϵ, then the resulting system is completely integrable. In fact we can see immediately that the quantities

$$R = (|A_1|^2 + |A_2|^2)^{\frac{1}{2}}, \quad K = \frac{(A_2\bar{A}_1^2 + A_1^2\bar{A}_2)}{2R^3} \tag{6.11}$$

are both constants of the motion. If we use the quantities ρ, σ, χ of (5.3), (5.4) then we may write

$$\left.\begin{aligned} \rho &= R\cos\beta, \\ \sigma &= R\sin\beta, \end{aligned}\right\} \quad K = \cos^2\beta\sin\beta\sin\chi. \tag{6.12}$$

Figure 6 shows curves of constant K. For fixed R they clearly define periodic solutions for β (and hence for ρ, σ) and χ, and we expect that of this two-parameter family of modulated waves a finite number will survive when the $O(\epsilon)$-terms are

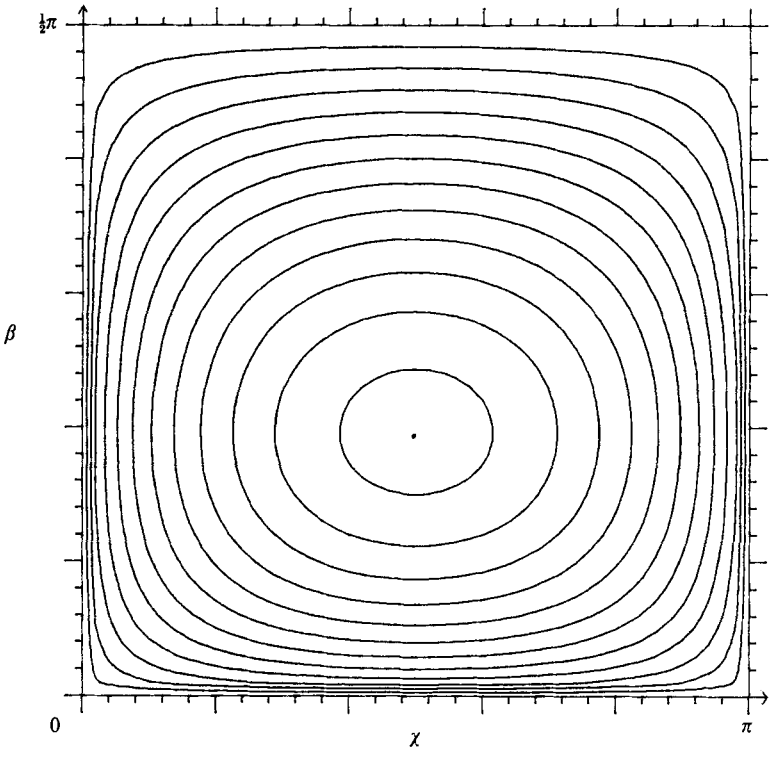

FIGURE 6. Contours of constant K (equations (6.11), (6.12)).

included in (6.10). In order to apply perturbation theory we need to ascertain the evolution of β and χ on curves of constant K. From (5.3), (5.4), (6.12) we have (with $\epsilon = 0$), $\dot{\rho} = -R \sin\beta\dot{\beta}$, so that

$$\left.\begin{aligned} \dot{\beta} &= -\alpha R \cos\beta \cos\chi, \\ \dot{\chi} &= \alpha R\left(\frac{\cos^2\beta}{\sin\beta} - 2\sin\beta\right)\sin\chi. \end{aligned}\right\} \tag{6.13a,b}$$

Eliminating $\cos\chi$ from (6.13a) using the definition of K we obtain

$$\dot{\beta}^2 = \alpha^2 R^2 \cos^2\beta(1 - K^2 \operatorname{cosec}^2\beta \sec^4\beta). \tag{6.14}$$

Letting $h \equiv \cos^2\beta$, $(\partial/\partial t = 2\alpha R(\partial/\partial\tau)$, we obtain (6.14) in the canonical form

$$h_\tau^2 = h^2 - h^3 - K^2. \tag{6.15}$$

This equation can be solved in terms of elliptic functions, but the results are not particularly illuminating. We prefer to write it in the form $\frac{1}{2}h_\tau^2 + \frac{1}{2}(h^3 - h^2) = -\frac{1}{2}K^2$, and regard $-\frac{1}{2}K^2$ as the energy of a particle in the potential $V(h) = \frac{1}{2}(h^3 - h^2)$. Clearly periodic orbits are possible with $h < 1$, for values of K^2 ranging from 4/27 (for which $h = \frac{2}{3}$) up to $K^2 = 0$, representing a homoclinic orbit of infinite period connecting the two fixed points given by $\sin\chi = 0$, $\beta = \frac{1}{2}\pi$; these are of course both to be identified with the pure-mode solution $A_1 = 0$, $A_2 \neq 0$. (The other apparent pair of fixed points at $\beta = 0$ is illusory as can be seen from examination of (6.13b). The difficulty stems from the singularity of the amplitude/phase representation at points where one of the complex amplitudes passes through zero.)

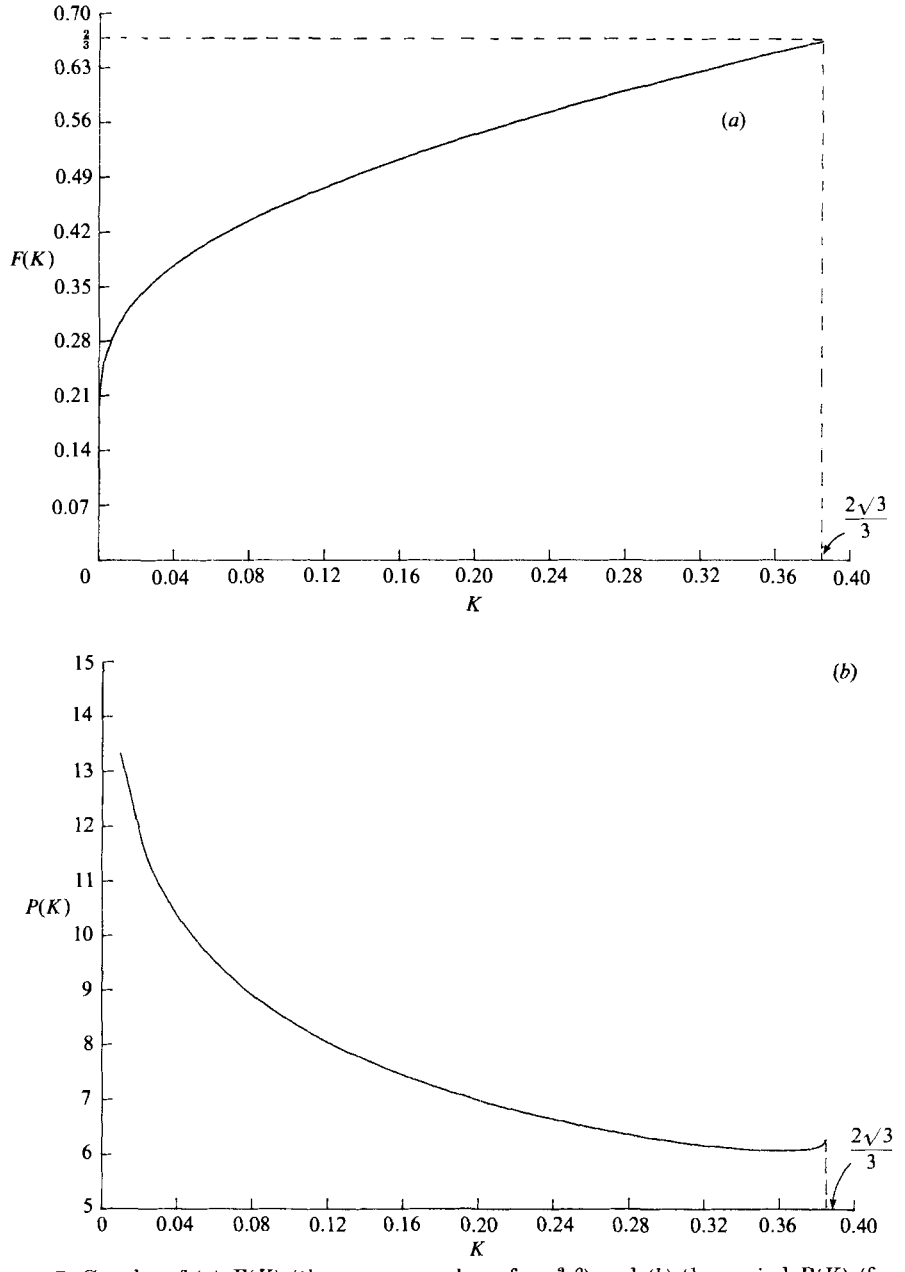

FIGURE 7. Graphs of (*a*) $F(K)$ (the average value of $\cos^2\beta$) and (*b*) the period $P(K)$ (for units in which $2\alpha R = 1$) for the modulated waves.

For any value of K^2 between 4/27 and 0 we may define h_1, h_2 ($h_1 < h_2$) as the two positive roots of the equation

$$h^2 - h^3 - K^2 = 0. \tag{6.16}$$

Then the period P of the modulation (with respect to the timescale τ) is given by

$$P(K) = 2\int_{h_1}^{h_2} \frac{\mathrm{d}h}{|h_\tau|}. \tag{6.17}$$

P is a function of K alone, and in terms of the original timescale the period is $(P(K)/2\alpha R)$: it is plotted in figure 7 together with the average value of h over the period, denoted by $F(K)$, and defined by

$$\langle h\rangle = \frac{2}{P(K)}\int_{h_1}^{h_2}\frac{h\,\mathrm{d}h}{|h_\tau|} \equiv F(K). \tag{6.18}$$

In what follows we shall also require the quantities

$$\langle\cos^4\beta\rangle = \langle h^2\rangle, \tag{6.19a}$$

$$\langle\sin^2\beta\rangle = 1-\langle h\rangle, \tag{6.19b}$$

$$\langle\sin^2\beta\cos^2\beta\rangle = \langle h\rangle-\langle h^2\rangle, \tag{6.19c}$$

$$\langle\sin^4\beta\rangle = 1-2\langle h\rangle+\langle h^2\rangle. \tag{6.19d}$$

All these integrals can be expressed in terms of $F(K)$. In fact

$$P(K)\,(2\langle h\rangle-3\langle h^2\rangle) = 2\int_{h_1}^{h_2}\frac{(2h-3h^2)\,\mathrm{d}h}{(h^2-h^3-K^2)^{\frac{1}{2}}} = 4[(h^2-h^3-K^2)^{\frac{1}{2}}]_{h_1}^{h_2} = 0 \tag{6.20}$$

so that

$$\langle\cos^4\beta\rangle = \tfrac{2}{3}F(K), \tag{6.21a}$$

$$\langle\sin^2\beta\rangle = 1-F(K), \tag{6.21b}$$

$$\langle\sin^2\beta\cos^2\beta\rangle = \tfrac{1}{3}F(K), \tag{6.21c}$$

$$\langle\sin^4\beta\rangle = 1-\tfrac{4}{3}F(K). \tag{6.21d}$$

From the figure it can be seen that $F(K)$ is a monotonic function of K, rising from near zero when $K \approx 0$ to a maximum of $2/3$ when $K^2 = 4/27$.

In order to find which of the above orbits approximate to periodic solutions of the full equations, we need to consider the $O(\epsilon)$-terms in (6.10). It is convenient to express these equations in terms of the three variables R, K and β, so that R and K will evolve on a slow timescale $T = \epsilon t$ when the small terms are considered. After some manipulation we arrive at the *exact* equations

$$\dot{R} = \epsilon R\{\mu_1\cos^2\beta+\mu_2\sin^2\beta-R^2[a_1\cos^4\beta+(b_1+b_2)\sin^2\beta\cos^2\beta+a_2\sin^4\beta]\}, \tag{6.22a}$$

$$\dot{K} = \epsilon K\,(\cos^2\beta-2\sin^2\beta)\{\mu_2-\mu_1+R^2[(a_1-b_2)\cos^2\beta+(b_1-a_2)\sin^2\beta]\}. \tag{6.22b}$$

In order to find the slow variations in R and K we may, correct to $O(\epsilon)$ take averages of $\cos^2\beta$, $\sin^2\beta$, etc. over the fast timescale, and regard β as satisfying (6.14) while we do so; then the equations for the evolution of R and K are, using (6.21),

$$R_T = R\{\mu_1 F(K)+\mu_2[1-F(K)]-\tfrac{1}{3}R^2[2a_1F(K)+(b_1+b_2)\,F(K)+a_2(3-4F(K))]\}, \tag{6.23}$$

and

$$K_T = K[3F(K)-2]\,[\mu_2-\mu_1+R^2(b_1-a_2)]. \tag{6.24}$$

The second-order system (6.23), (6.24) controls the slow evolution of the modulations to the travelling waves. Fixed points correspond to limit cycles, i.e. modulated waves with constant modulation frequency.

These fixed points are of two types:

(1) $$3F = 2, \quad \mu_1+2\mu_2-\tfrac{1}{3}R^2\Delta = 0. \tag{6.25}$$

These have $K^2 = 4/27$ and so are the travelling waves, which are in fact given without approximation by (6.25).

(2) $3F \neq 2$; then we have

$$\left.\begin{aligned} \mu_2-\mu_1+R^2(b_1-a_2) &= 0, \\ \mu_1 F+\mu_2(1-F) &= \tfrac{1}{3}R^2[2a_1F+(b_1+b_2)F+a_2(3-4F)]. \end{aligned}\right\} \quad (6.26a,b)$$

These represent modulated waves. The solutions (6.26) bifurcate from the travelling waves when $F = \frac{2}{3}$ in (6.26); that is, when

$$3(2\mu_1+\mu_2) = \frac{(\mu_2-\mu_1)\Delta}{a_2-b_1}. \quad (6.27)$$

This line can be shown to coincide, in the limit of large α or small μ_i, with the exact condition for Hopf bifurcation given by (5.15).

For each value of $K^2 < 4/27$, (6.26) defines a line in the (μ_1, μ_2)-plane. It is easily established, since $F(K)$ is monotonic, that each value of K defines a unique line, so the domain in which modulated waves exist lies wholly on one side of the bifurcation curve (6.27), at least sufficiently close to the origin. Thus the stability of these waves can be decided by finding the location of the line corresponding to the maximum amplitude of modulation, namely when $K \approx 0$, $F \approx 0$. This gives

$$\mu_2 = R^2a_2, \quad \mu_2-\mu_1+R^2(b_1-a_2) = 0. \quad (6.28)$$

Thus for $F = 0$, $\mu_1/\mu_2 = b_1/a_2$, while on the Hopf line (from (6.27))

$$\mu_1/\mu_2 = (c+b_1)/(c+a_2),$$

where $c = \frac{2}{9}(2a_1-2b_1+b_2-a_2)$. Since the region of *stable* travelling waves has μ_1/μ_2 larger than its value on the Hopf line, we can see that modulated waves will only be stable (in the case $a_2 > 0, c+a_2 > 0$ which obtains for our experiment) if $c > 0, a_2 > b_1$. A full stability analysis confirms these results, and demonstrates the non-existence of a Hopf bifurcation of the system (6.23), (6.24), which would lead to a *quasi-periodic* modulation if it existed, except for some very exotic combinations of parameters.

6.3. *The homoclinic orbit*

We have already noted in §5 that the mixed-mode branch M_+ suffers a Hopf bifurcation on the line given by (5.10). This bifurcation is subcritical for values of the parameters appropriate to the experiment described in earlier sections, and leads to growing oscillations of the amplitudes ρ and σ. As the amplitude of the waves increases, the phase χ initially stays close to its original value 0 but eventually σ becomes very small on part of the trajectory. It can then be seen from (5.4) that $\chi = 0$ will be strongly unstable in this region, and in fact χ will change from ≈ 0 to $\approx \pi$ in a short time. (This is equivalent to A_2 passing through zero.) Once this change in χ has taken place the only solution stable with respect to amplitude is the pure mode $\rho = 0, \sigma^2 = \mu_2/a_2$. Thus ρ will become very small and $\sigma \to (\mu_2/a_2)^{\frac{1}{2}}$, so that $\chi = \pi$ will be unstable again. Thus χ changes slowly from $\approx \pi$ to ≈ 0, when there is again instability with respect to amplitude and the cycle repeats as before, except that on each circuit the period will (typically) increase since χ becomes closer and closer to 0 or π in appropriate parts of the trajectory. The system thus tends to approach a homoclinic orbit, formed by the line $\rho = 0$, $\sigma = (\mu_2/a_2)^{\frac{1}{2}}$, $0 \leqslant \chi \leqslant \pi$, together with a trajectory that may be best described by allowing σ to take negative values, and making the identification $(\sigma, \chi) \to (-\sigma, \pi+\chi)$. Then the trajectory joins $\sigma = +(\mu_2/a_2)^{\frac{1}{2}}$ with $\sigma = -(\mu_2/a_2)^{\frac{1}{2}}$ at $\chi = 0$. It is remarkable that this orbit remains attracting within a finite region of (μ_1, μ_2), in contrast to the homoclinic and

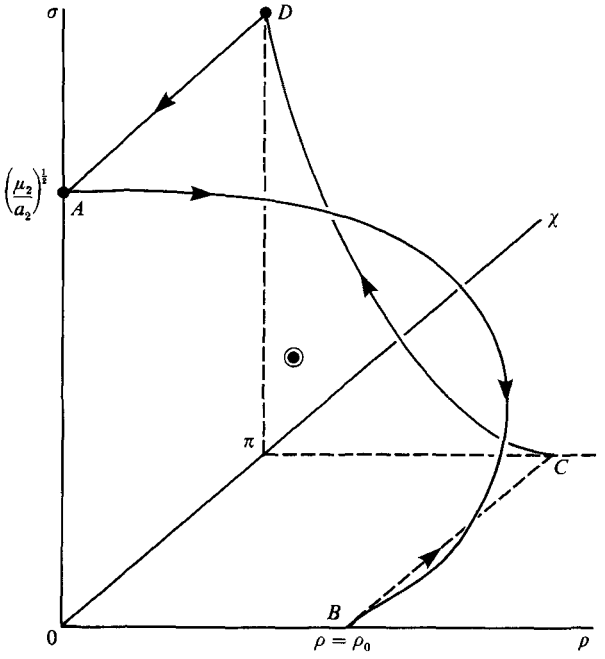

FIGURE 8. Sketch of the structurally stable homoclinic orbit in (ρ, σ, χ)-space. The orbit is traversed in the direction shown by the arrows. The dotted portion of the orbit is traversed instantaneously since A_2 changes sign there. The circled dot denotes the mixed-mode solution M_+.

heteroclinic orbits that appear in many multiple bifurcation problems (see, among many examples, Knoblich & Proctor 1981). This is because all parts of the orbit lie in invariant planes. Figure 8 shows how ρ and σ vary during an approach to the orbit.

The dynamics near the homoclinic orbit are governed by (5.3a, c) and (5.4). We can divide the orbit into four regions, illustrated in figure 8, and coupled by asymptotic matching. In what follows ϵ is a small parameter.

(i) $\sigma = O(\epsilon)$; $\rho \approx \rho_0$ a constant, and χ changes from being close to O to being close to π in a time $O(\epsilon)$.

(ii) χ is close to π, so $\chi = \pi - \epsilon\tilde{\chi}$; σ and ρ are $O(1)$ and vary from $\rho \approx \rho_0$, $\sigma \approx 0$ on entry to $\rho \approx 0$, $s \approx \sigma_0 = (\mu_2/a_2)^{\frac{1}{2}}$ in a time $O(1)$.

(iii) ρ is small, $\sigma \approx \sigma_0$ and χ decreases from $\approx \pi$ to ≈ 0 in a time $O[\ln(1/\epsilon)]$.

(iv) χ is $O(\epsilon)$, σ and ρ are $O(1)$ and vary from $\rho \approx 0$, $\sigma \approx \sigma_0$ to $\rho \approx \rho_0$, $\sigma \approx 0$ in a time $O(1)$.

No complete analytical results are possible for regions (ii) and (iv) except in certain limiting cases, but useful information can still be obtained. We begin the analysis by considering region (i), and choose scaled variables by defining

$$t = \epsilon\tau, \quad \sigma = \epsilon\tilde{\sigma}. \tag{6.29}$$

$\rho \approx \rho_0$ throughout this region (ρ_0 is not known at this stage), so (5.3), (5.4) may be reduced to

$$\frac{\mathrm{d}\tilde{\sigma}}{\mathrm{d}\tau} = -\alpha\rho_0^2 \cos\chi + O(\epsilon), \quad \frac{\mathrm{d}\chi}{\mathrm{d}\tau} = \alpha\frac{\rho_0^2}{\tilde{\sigma}} \sin\chi + O(\epsilon). \tag{6.30}$$

These two equations can be combined to give

$$\frac{\mathrm{d}}{\mathrm{d}\tau}(\tilde{\sigma}\,\mathrm{e}^{\mathrm{i}\chi}) = -\alpha\rho_0^2 \tag{6.31}$$

$$\left.\begin{aligned}\tilde{\sigma}\cos\chi &= -\alpha\rho_0^2\tau + \text{const},\\ \tilde{\sigma}\sin\chi &= \text{const}.\end{aligned}\right\} \tag{6.32}$$

If we choose $t = 0$ to be the moment when $\chi = \frac{1}{2}\pi$, and let $\tilde{\sigma}\sin\chi = A_1$, then

$$\tilde{\sigma} = A_1\left(1+\left(\frac{\alpha\rho_0^2\tau}{A_1}\right)^2\right)^{\frac{1}{2}} \tag{6.33}$$

and thus for large $|\tau|$, we may write in terms of the outer variables

$$\sigma \sim \alpha\rho_0^2|t|, \qquad \tau\to\pm\infty, \tag{6.34a}$$

$$\chi \sim \frac{-\epsilon A_1}{\alpha\rho_0^2 t}, \qquad \tau\to-\infty, \tag{6.34b}$$

$$\sim\pi-\frac{\epsilon A_1}{\alpha\rho_0^2 t}, \qquad \tau\to+\infty. \tag{6.34c}$$

In region (ii), we let $\chi = \pi-\epsilon\tilde{\chi}$; then, at leading order we get

$$\frac{\mathrm{d}\rho}{\mathrm{d}t} = -\alpha\rho\sigma+\mu_1\rho-a_1\rho^3-b_1\sigma^2\rho, \tag{6.35a}$$

$$\frac{\mathrm{d}\sigma}{\mathrm{d}t} = \alpha\rho^2+\mu_2\sigma-a_2\sigma^3-b_2\sigma\rho^2, \tag{6.35b}$$

$$\frac{\mathrm{d}\tilde{\chi}}{\mathrm{d}t} = \alpha\left(2\sigma-\frac{\rho^2}{\sigma}\right)\tilde{\chi}. \tag{6.35c}$$

The first two equations may be solved separately with initial conditions (at $t = 0$) $\rho = \rho_0$, $\sigma = 0$. This solution curve will end at the point $\rho = 0$, $\sigma = \sigma_0$. The trajectory may be characterized by the relation between ρ and σ, which is not known in closed form, but is governed by

$$\frac{\mathrm{d}\sigma}{\mathrm{d}\rho} = \frac{\alpha\rho^2+\mu_2\sigma-a_2\sigma^3-b_2\sigma\rho^2}{-\alpha\rho\sigma+\mu_1\rho-a_1\rho^3-b_1\rho\sigma^2}. \tag{6.36}$$

whose solution we denote by $\sigma = \sigma_1(\rho)$. Once σ_1 is known, σ and ρ may be found as functions of time: the expression giving ρ is

$$t = \int_\rho^{\rho_0}\frac{\mathrm{d}\rho'}{\alpha\rho'\sigma-\mu_1\rho'+a_1\rho'^3+b_1\sigma^2\rho'}. \tag{6.37}$$

As $\rho\to 0$ in (6.37) the integral becomes singular. We can exploit this by putting (6.37) in the equivalent form

$$\rho = \rho_0\exp(\mu_1-\alpha\sigma_0-b_1\sigma_0^2)\exp\left\{\int_\rho^{\rho_0}\frac{\mathrm{d}\rho'}{\rho'}\left[\frac{\alpha\sigma_0+b_1\rho_0^2-\mu_1}{\alpha\sigma-\mu_1+a_1\rho'^2+b_1\sigma^2}-1\right]\right\}, \tag{6.38}$$

Equation (6.35*b*) can be then formally solved, determining the coefficient by matching to (6.34*b*), to yield

$$\tilde{\chi} = \frac{A_1}{\alpha\rho_0^2 t}\exp\left\{\int_0^t \left(2\sigma - \frac{\alpha\rho^2}{\sigma} + \frac{1}{t'}\right)\mathrm{d}t'\right\}, \tag{6.39}$$

where $\rho(t')$ id determined by (6.38) and $\sigma = \sigma_1[\rho(t')]$.

Now as $t \to \infty$, $\sigma \to \sigma_0$ and $\rho \to 0$, so from (6.39)

$$\tilde{\chi} \sim \frac{A_1 I_1}{\alpha\rho_0^2}\exp(2\alpha\sigma_0 t), \quad t \to \infty, \tag{6.40}$$

where
$$I_1 = \lim_{t\to\infty}\exp\left\{\int_0^t \left[2\alpha(\sigma-\sigma_0) - \frac{\alpha\rho^2}{\sigma} + \frac{1}{t'}\right]\mathrm{d}t' - \ln t\right\},$$

where I_1 is finite, since $\sigma - \sigma_0$ and ρ^2 decay exponentially as $t \to \infty$. The evolution of ρ as a function of t may be deduced from (6.38):

$$\rho \sim \rho_0 I_2 \exp(\mu_1 - \alpha\sigma_0 - b_1\sigma_0^2)t, \tag{6.41a}$$

where
$$I_2 = \exp\left\{\int_0^{\rho_0}\left[\frac{\alpha\sigma_0 + b_1\sigma_0^2 - \mu_1}{\alpha\sigma - \mu_1 + a_1\rho^2 + b_1\sigma^2} - 1\right]\frac{\mathrm{d}\rho}{\rho}\right\}. \tag{6.41b}$$

Again, I_2 is finite, because the term in square brackets is $O(\epsilon)$ near $\rho = 0$.

In region (iii), $\sigma \approx \sigma_0$, so we may write, ignoring quadratic and higher powers of ρ,

$$\frac{\mathrm{d}\rho}{\mathrm{d}t} = \alpha\sigma_0\rho\cos\chi + \mu_1\rho - b_1\rho\sigma_0^2, \tag{6.42a}$$

$$\frac{\mathrm{d}\chi}{\mathrm{d}t} = -2\alpha\sigma_0\sin\chi. \tag{6.42b}$$

We can solve these equations to yield

$$\cot\tfrac{1}{2}\chi = \exp[2\alpha\sigma_0(t-c_1)], \tag{6.43a}$$

$$\rho^2 = c_2\cosh[2\alpha\sigma_0(t-c_1)]\exp[2(\mu_1 - b_1\sigma_0^2)t], \tag{6.43b}$$

where the constants c_1 and c_2 are to be determined by matching with region (ii). As $t - c_1 \to -\infty$, $\chi \sim \pi - 2\exp[2\alpha\sigma_0(t-c_1)]$ and so by comparison with (6.40)

$$c_1 = -\frac{1}{2\alpha\sigma}\ln\left[\frac{\epsilon A_1 I_1}{2\alpha\rho_0^2}\right]. \tag{6.44}$$

From (6.43*b*) $\rho \sim (\frac{1}{2}c_2)^{\frac{1}{2}}\exp(\alpha\sigma_0 c_1)\exp[(\mu_1 - b_1\sigma_0^2 - \alpha\sigma_0)t]$ as $t - c_1 \to -\infty$, so to match with (6.41*a*),

$$\rho_0 I_2 = (\tfrac{1}{2}c_2)^{\frac{1}{2}}\exp(\alpha\sigma_0 c_1) \tag{6.45a}$$

or
$$c_2 = \frac{\epsilon I_2^2 I_1 A_1}{\alpha}. \tag{6.45b}$$

The minimum value of ρ given by (6.43*b*) at $t = c_1$ is then a positive power of ϵ provided $\mu_1 - \alpha\sigma_0 - b_1\sigma_0^2 < 0$, thus justifying the neglect of higher powers of ρ in (6.42). For $t - c_1 \to \infty$,

$$\chi \sim 2\exp(-2\alpha\sigma_0(t-c_1)], \tag{6.46a}$$

$$\rho \sim (\tfrac{1}{2}c_2)^{\frac{1}{2}}\exp[\alpha\sigma_0(t-c_1)]\exp(\mu_1 - b_1\sigma_0^2)t \tag{6.46b}$$

so that $\chi \to 0$ and ρ becomes large. In region (iv) $\chi = \epsilon\tilde{\chi}$ is small. The equations in this region are

$$\frac{\mathrm{d}\rho}{\mathrm{d}t} = \alpha\rho\sigma + \mu_1\rho - a_1\rho^3 - b_1\rho\sigma^2, \tag{6.47a}$$

$$\frac{\mathrm{d}\sigma}{\mathrm{d}t} = -\alpha\rho^2 + \mu_2\sigma - a_2\sigma^3 - b_2\sigma\rho^2, \tag{6.47b}$$

$$\frac{\mathrm{d}\tilde{\chi}}{\mathrm{d}t} = \alpha\left(\frac{\rho^2}{\sigma} - 2\sigma\right)\tilde{\chi} \tag{6.47c}$$

and, as in region (ii), we seek the trajectory that goes from $\sigma \approx \sigma_0$, $\rho \approx 0$ to $\sigma \approx 0$, $\rho \approx \rho_0$. As in that case, we have no analytical solution for the trajectories, but we can suppose that $\rho = \rho(\sigma)$ is known. Since the point $\sigma = \sigma_0$, $\rho = 0$ is a saddle point, there is only one trajectory passing through it (apart from $\rho(t) = 0$) and so $\rho_0 = \rho(0)$ is uniquely determined.

Solving (6.47c) for $\tilde{\chi}$ yields

$$\tilde{\chi} = c_3 \exp\left(-2\alpha\sigma_0 t\right) \exp\left\{\int_{-\infty}^{t}\left[\frac{\alpha\rho^2}{\sigma} - 2\alpha(\sigma-\sigma_0)\right]\mathrm{d}t'\right\} \tag{6.48}$$

and by comparing (6.48) with (6.46a) we arrive at the result

$$\tilde{\chi} = \frac{2}{\epsilon}\exp\left(-2\alpha\sigma_0(t-c_1)\right)\exp\left\{\int_{-\infty}^{t}\left(\frac{\alpha\rho^2}{\sigma} - 2\alpha(\sigma-\sigma_0)\right)\mathrm{d}t'\right\} \tag{6.49}$$

since the integrand $\to 0$ as $t \to -\infty$. A similar analysis for ρ (compare (6.38)) yields

$$\rho = (\tfrac{1}{2}c_2)^{\frac{1}{2}}\exp\left[\alpha\sigma_0(t-c_1)\right]\exp\left(\mu_1 - b_1\sigma_0^2\right)t\exp\left\{\int_0^{\rho}\frac{1}{\rho}\left[\frac{\alpha\sigma_0+\mu_1-b_1\sigma_0^2}{\alpha\sigma+\mu_1-b_1\sigma^2-a_1\rho^2}-1\right]\mathrm{d}\rho\right\} \tag{6.50}$$

with $\sigma = \sigma(\rho)$ in the exponential integrand.

We can now determine the time at which ρ returns to its starting value, ρ_0. If the elapsed time is T, then T is given by matching the $t \to \infty$ limit of (6.50) to ρ_0,

$$\rho_0 = I_3(\tfrac{1}{2}c_2)^{\frac{1}{2}}\exp\left(-\alpha\sigma_0 c_1\right)\exp\left[\left(\mu_1 - b_1\sigma_0^2 + \alpha\sigma_0\right)T\right] \tag{6.51a}$$

where

$$I_3 = \exp\left\{\int_0^{\rho_0}\frac{1}{\rho}\left(\frac{\alpha\sigma_0+\mu_1-b_1\sigma_0^2}{\alpha\sigma+\mu_1-b_1\sigma^2-a_1\rho^2}-1\right)\mathrm{d}\rho\right\}. \tag{6.51b}$$

On the second entry to region (i) we have, by comparison with (6.45)

$$\left.\begin{aligned}\sigma &\sim \alpha\rho_0^2|t-\tau| \\ \chi &\sim \frac{\epsilon A_2}{\alpha\rho_0^2}\frac{1}{T-t}\end{aligned}\right\} \quad \text{as } t \to T^-, \tag{6.52}$$

where, for stability of the homoclinic orbit, $|A_2| < |A_1|$. We obtain an expression for χ from (6.49):

$$\chi = \frac{2\exp\left(-2\alpha\sigma_0(t-c_1)\right)}{T-t}\lim_{t_0\to-\infty}\exp\left\{\int_{t_0}^{t}\left(\frac{\alpha\rho^2}{\sigma} - 2\alpha(\sigma-\sigma_0) - \frac{1}{T-t'}\right)\mathrm{d}t' + \ln\left(T-t_0\right)\right\} \tag{6.53}$$

where the quantity in curly brackets remains finite as $t \to T^-$. Hence we have as $t \to T^-$

$$\chi \sim \frac{2I_4}{T-t} \exp\{-2\alpha\sigma_0(T-c_1)\} = \frac{\epsilon A_2}{\alpha\rho_0^2(T-t)},$$

where
$$I_4 = \lim_{t_0 \to -\infty} \exp\left\{\int_{t_0}^{T}\left[\frac{\alpha\rho^2}{\sigma} - 2\alpha(\sigma-\sigma_0) - \frac{1}{T-t'}\right] dt' + \ln(T-t_0)\right\} \tag{6.54}$$

so that
$$A_2\epsilon = 2\alpha\rho_0^2 I_4 \exp[-2\alpha\sigma_0(T-c_1)]. \tag{6.55}$$

We can now determine A_2/A_1. Using (6.44), (6.45), (6.51*a*) and (6.55) we find

$$T = (a\sigma_0 + \mu_1 - b_1\sigma_0^2)^{-1} \ln\left(\frac{2\alpha\rho_0^2}{\epsilon A_1 I_1 I_2 I_3}\right) \tag{6.56}$$

and
$$A_2\epsilon \frac{4\alpha^2\rho_0^4 I_4}{I_1}\left(\frac{I_1 I_2 I_3}{2\alpha\rho_0^2}\right)^{\lambda} (\epsilon A_1)^{\lambda-1}. \tag{6.57}$$

where $\lambda = 2\alpha\sigma_0/(\mu_1 - b_1\sigma_0^2 + \alpha\sigma_0^2)$. Now this can be written

$$\frac{A_2}{A_1} = \frac{4\alpha^2\rho_0^4 I_4}{I_1}\left(\frac{I_1 I_2 I_3}{2\alpha\rho_0^2}\right)^{\lambda} A_1^{\lambda-2}\epsilon^{\lambda-2} = K\epsilon^{\lambda-2}, \tag{6.58}$$

where K is a number of order unity. If ϵ is small, the criterion that $A_2/A_1 < 1$ is that $\lambda > 2$, for if this condition holds $\epsilon^{\lambda-2}$ will dominate K at sufficiently small ϵ. So the criterion for stability of the orbit is

$$\lambda > 2 \quad \text{or} \quad \mu_1 < \frac{b_1\mu_2}{a_2}. \tag{6.59}$$

For small ϵ the ratio of the periods for each 'pulse' of the trajectory is

$$\frac{T_2}{T_1} \sim \frac{\ln \epsilon A_2}{\ln \epsilon A_1} \sim (\lambda - 1). \tag{6.60}$$

The conditions required for the homoclinic orbit to exist and be stable are: (i) $\mu_1 - \alpha\sigma_0 - b_1\sigma_0^2 < 0$ so that ρ becomes small with $\chi \approx \pi$ as the singular point $\rho = 0$, $\sigma = \sigma_0$ is approached: (ii) $\mu_1 + \alpha\sigma_0 - b_1\sigma_0^2 > 0$, so that the singular point is unstable when $\chi \approx 0$: (iii) $\mu_1 - b_1\sigma_0^2 < 0$ for the homoclinic orbit to be stable. These conditions are all satisfied if

$$0 > \mu_1 - \frac{b_1\mu_2}{a_2} > -\alpha\left(\frac{\mu_2}{a_2}\right)^{\frac{1}{2}}. \tag{6.61}$$

Note that the boundary of the stability region coincides with the line in (μ_1, μ_2)-space that gives the locus of the homoclinic orbit arising from the Hopf bifurcation of the travelling-wave solutions (see (6.31) and ff.). Thus there is an unusual global bifurcation on this line, the nature of which is not fully understood.† It is remarkable that the stability criterion (6.62) does not involve the details of the 'pulsed' section of the orbit: this is because the time spent on this phase is very short compared with that for $\rho \approx 0$. The behaviour of ρ and σ as functions of time during the approach to the homoclinic orbit are shown in figure 9.

† An elegant representation of the orbit that clarifies the dynamics and illuminates the nature of the bifurcation that arises on this boundary has recently been given by J. W. Swift (1988, private communication).

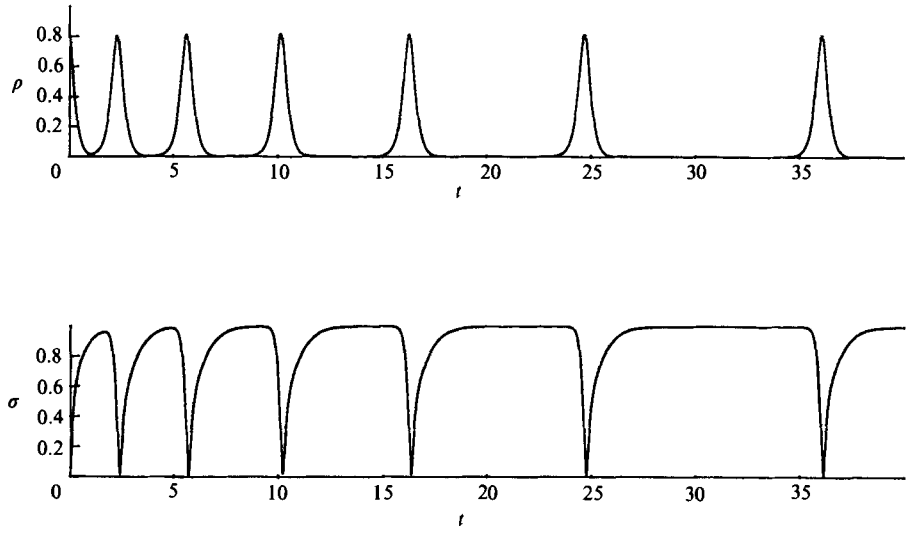

FIGURE 9. The approach to the homoclinic orbit, ρ and σ *vs.* time under system (5.1) with $a_1 = a_2 = 1$, $b_1 = b_2 = 0$, $\mu_1 = -0.8$, $\mu_2 = 1.0$, $\alpha = 5$.

6.4. *The effect of imperfections on the homoclinic orbit*

While the homoclinic orbit described above is structurally stable to changes in the parameters in (5.1), it does not survive the addition of terms that lead to imperfect bifurcations, rather than perfect ones. In particular, if the surface $\rho = 0$ is no longer an invariant surface, the crucial part that it plays in the approach to the homoclinic orbit will change. We may model such behaviour by adding a term to (5.1*a*) to give

$$\dot{A}_1 = \beta + \mu_1 A_1 + \mathrm{i}\alpha A_2 \bar{A}_1 - a_1 A_1 |A_1|^2 - b_1 A_1 |A_2|^2, \tag{6.62}$$

where the constant β (which can be taken to be real and positive) represents the effect of external forcing of the mode $\propto \mathrm{e}^{\mathrm{i}kx}$. Such a term will (together with a similar one in (5.1 b) that we do not discuss here) give the dominant effect of a general external forcing on the motion. It is particularly pertinent to convection in a cylindrical geometry, where the horizontal coordinate x may be identified with the azimuthal angle θ, and where $k = 1$ gives an imperfection $\propto \mathrm{e}^{\mathrm{i}\theta}$, corresponding to the effect of tilting the cylinder slightly. For sufficiently small β, the effect of the imperfection on the travelling waves will be negligible (though the amplitude and speed of the waves will not be constant, but will vacillate slightly as the waves pass 'over the bump'). However, the effect of this term on the homoclinic orbit is crucial; numerical experiments have shown that with $\beta \neq 0$ the realized solution is *periodic*, close to the homoclinic orbit, with a period that increases as β decreases. These results are confirmed by the analysis below.

Using (6.62) instead of (5.1*a*) we get instead of (5.3*a*), (5.3*b*)

$$\dot{\rho} = \mu_1 \rho + \alpha\rho\sigma \cos\chi - a_1 \rho^3 - b_1 \rho\sigma^3 - b_1 \rho\sigma^2 + \beta \cos\theta, \tag{6.63a}$$

$$\rho\dot{\theta} = -\alpha\rho\sigma \sin\chi - \beta \sin\theta. \tag{6.63b}$$

The equations for σ and χ are

$$\dot{\sigma} = \mu_2 \sigma - \alpha\rho^2 \cos\chi - b_2 \rho^2 \sigma - a_2 \sigma^3, \tag{6.64a}$$

$$\dot{\chi} = \alpha\left(\frac{\rho^2}{\sigma} - 2\sigma\right)\sin\chi - \frac{2\beta\sin\theta}{\rho}. \tag{6.64b}$$

Numerical experiments have revealed that two types of periodic orbit are possible, which we denote by H_+ and H_-. The condition determining which orbit occurs emerges from the analysis. In what follows, the upper sign is associated with the H_+ case, and the lower sign with the H_- case. In each case, there are eight distinct asymptotic regions: fortunately, there is some symmetry which simplifies the analysis.

(i) $\sigma \sim O(\epsilon)$, $\rho \approx \rho_0$, $\theta \approx \frac{1}{2}\pi \mp \frac{3}{4}\pi$, χ varies from O to π.

(ii) $\sigma, \rho \sim O(1)$, $\theta \approx \frac{1}{2}\pi \mp \frac{3}{4}\pi$, $\chi = \pi - \epsilon\tilde{\chi}$. In the H_+ case, $\tilde{\chi}$ changes sign in this regime, starting positive and ending negative. In the H_- case, $\tilde{\chi}$ remains positive.

(iii) $\sigma \approx \sigma_0$, ρ small, θ changes from $\frac{1}{2}\pi \mp \frac{3}{4}\pi$ to $\frac{1}{2}\pi \mp \frac{1}{4}\pi$, χ changes from π to $\pi \pm \pi$.

(iv) $\sigma, \rho \sim O(1)$, $\theta \approx \frac{1}{2}\pi \mp \frac{1}{4}\pi$, $\chi = \epsilon\tilde{\chi}$. In the H_+ case, $\tilde{\chi}$ is negative throughout. In the H_- case, $\tilde{\chi}$ changes sign, being positive on entry and negative on exit.

(v) $\sigma \sim O(\epsilon)$, $\rho \approx \rho_0$, $\theta \simeq \frac{1}{2}\pi \mp \frac{1}{4}\pi$, χ varies from 2π to π.

(vi) $\sigma, \rho \sim O(1)$, $\theta \approx \frac{1}{2}\pi \mp \frac{1}{4}\pi$, $\chi = \pi + \epsilon\tilde{\chi}$. In the H_+ case, $\tilde{\chi}$ starts positive and ends negative. In the H_- case $\tilde{\chi}$ remains positive.

(vii) $\sigma \approx \sigma_0$, ρ small, θ changes from $\frac{1}{2}\pi \mp \frac{1}{4}\pi$ to $\frac{1}{2}\pi \mp \frac{3}{4}\pi$, χ varies from π to $\pi \mp \pi$.

(viii) $\sigma, \rho \sim O(1)$, $\theta \approx \frac{1}{2}\pi \mp \frac{3}{4}\pi$, $\chi = \epsilon\tilde{\chi}$. In the H_+ case, $\tilde{\chi}$ is positive throughout. In the H_- case, $\tilde{\chi}$ is negative on entry, positive on exit.

In both cases, on exit from region (viii) we re-enter region (i). The behaviour in regions (v)–(viii) is the same as in regions (i)–(iv) apart from some sign changes. The parameter β is taken to be $O(\epsilon)$, so we set $\beta = \epsilon\hat{\beta}$. The notation adopted is the same as in §6.3.

Region (i) is governed by (6.30), since the β-terms make no contribution to this region. The solutions (6.32), (6.33) hold, and the asymptotic results (6.34) are valid.

Region (ii) is slightly changed (the even-numbered regions are all changed, the odd-numbered regions are governed by original leading-order equations).

$$\left.\begin{aligned} \frac{\mathrm{d}\rho}{\mathrm{d}t} &= -\alpha\rho\sigma + \mu_1\rho - a_1\rho^3 - b_1\sigma^2\rho, \\ \frac{\mathrm{d}\sigma}{\mathrm{d}t} &= \alpha\rho^2 + \mu_2\sigma - a_2\sigma^3 - b_2\sigma\rho^2 \end{aligned}\right\} \tag{6.65}$$

as before, but

$$\frac{\mathrm{d}\tilde{\chi}}{\mathrm{d}t} = \alpha\left(2\sigma - \frac{\rho^2}{\sigma}\right)\tilde{\chi} - \frac{\sqrt{2}\hat{\beta}}{\rho}. \tag{6.66}$$

The $\rho - \sigma$ and $\rho(t)$ relations are again governed by (6.36), (6.37) and (6.38), as before. But now

$$\tilde{\chi} = \frac{A_1}{\alpha\rho_0^2}\exp\left\{\int_0^t\left(2\alpha\sigma - \frac{\alpha\rho^2}{\sigma} + \frac{1}{t'}\right)\mathrm{d}t'\right\} - \frac{1}{t}\exp\left\{\int_0^t\left(2\alpha\sigma - \frac{\alpha\rho^2}{\sigma} + \frac{1}{t'}\right)\mathrm{d}t'\right\}$$
$$\times\left[\int_0^t \frac{\hat{\beta}\sqrt{2}}{\rho}\, t' \exp\left\{\int_0^t\left(-2\alpha\sigma + \frac{\alpha\rho^2}{\sigma} - \frac{1}{t''}\right)\mathrm{d}t''\right\}\mathrm{d}t'\right]. \tag{6.67}$$

As $t \to 0$, the term in square brackets is $O(t^2)$, so this expression matches onto (6.34c) satisfactorily. But the extra term makes an important contribution to the $t \to \infty$ behaviour, so (6.40) is replaced by

$$\tilde{\chi} \sim \frac{A_1}{\alpha\rho_0^2} I_1 \exp(2\alpha\sigma_0 t) - I_1 \hat{\beta} J_1 \exp(2\alpha\sigma_0 t), \tag{6.68}$$

where
$$I_1 = \lim_{t\to\infty} \exp\left\{\int_0^t \left(2\alpha(\sigma-\sigma_0) - \frac{\alpha\rho^2}{\sigma} + \frac{1}{t'}\right) \mathrm{d}t' - \ln(t)\right\}$$

as before, and

$$J_1 = \lim_{t\to\infty} \int_0^t \frac{t'\sqrt{2}}{\rho} \exp(-2\alpha\sigma_0 t') \exp\left\{\int_0^{t'} \left[-2\alpha(\sigma-\sigma_0) + \frac{\alpha^2\rho}{\sigma} - \frac{1}{t''}\right] \mathrm{d}t''\right\} \mathrm{d}t'.$$

Like I_1, J_1 is a finite integral. The $t \to \infty$ behaviour of ρ is governed by (6.41) as before.

As $t \to \infty$, it may be that $\hat{\beta} J_1 > A_1/\alpha\rho_0^2$, in which case $\tilde{\chi}$ changes sign. This occurs in the H_+ case. Alternatively, $A_1/\alpha\rho_0^2 > \hat{\beta} J_1$ in which case $\tilde{\chi}$ remains positive, and we are in the H_- case. We cannot at this stage say which case we are in, as A_1 is not yet determined. It is interesting to note that it is the small changes in χ (the changes are only $O(\epsilon)$) in the even-numbered regions that control the large changes in χ in the odd-numbered regions.

We now enter region (iii). An important question is whether the term $2\beta \sin\theta/\rho$ should enter into the χ-equation here. From (6.43), (6.44) and (6.45) we find that the minimum value of ρ,

$$\rho_{\min} = \left(\frac{I_2^2 I_1 A_1}{\alpha}\right)^{\frac{1}{2}} \left(\frac{2\alpha\rho_0^2}{A_1 I_1}\right)^{(\mu_1 - b_1\sigma_0^2)/2\alpha\sigma_0} \epsilon^{(\alpha\sigma_0 + \mu_1 - b_1\sigma_0^2)/2\alpha\sigma_0}, \tag{6.69}$$

so provided $\mu_1 - b_1\sigma_0^2 - \alpha\sigma_0 < 0$, which is a condition for the existence of a homoclinic orbit, β/ρ is of order a positive power of ϵ and so the term $2\beta \sin\theta/\rho$ does not enter into the $\dot{\chi}$-equation. This is fortunate, since θ varies in this region, so the inclusion of the β-term would make the problem intractable.

So region (iii) is governed by (6.42) and solutions (6.43) apply, except that in the H_+ case $\cot\chi/2 = -\exp 2\alpha\sigma_1(t-c_1)$ is the relevant solution, but we must match onto (6.68) rather than (6.40a), so

$$c_1 = -\frac{1}{2\alpha\sigma_0} \ln\left[\mp\frac{\epsilon I_1}{2}\left(\frac{A_1}{\alpha\rho_0^2} - \hat{\beta} J_1\right)\right]. \tag{6.70}$$

Equation (6.45a) still holds, but the altered value of c_1 means that

$$c_2 = \mp\epsilon\rho_0^2 I_2^2 I_1 \left(\frac{A_1}{\alpha\rho_0^2} - \hat{\beta} J_1\right). \tag{6.71}$$

These values of c_1 and c_2 are the same order in ϵ as the previous values, justifying our neglect of the $2\beta \sin\theta/\rho$-term (and the quadratic terms in ρ).

With the revised values of c_1 and c_2, (6.46) holds for $t - c_1 \to \infty$. The change in χ from π to $\pi \pm \pi$ in region (iii) is achieved by θ changing by $\frac{1}{2}\pi$ from $\frac{1}{2}\pi \mp \frac{3}{4}\pi$ to $\frac{1}{2}\pi \mp \frac{1}{4}\pi$,

as can be seen by comparing (6.63*b*) with (6.42*b*). So we enter region (iv) with $\chi = \epsilon\tilde{\chi}$, $\theta \approx \frac{1}{2}\pi \mp \frac{1}{4}\pi$. The governing equations in this region are

$$\frac{\mathrm{d}\rho}{\mathrm{d}t} = \mu_1\rho + \alpha\sigma\rho - a_1\rho^3 - b_1\rho\sigma^2, \tag{6.72a}$$

$$\frac{\mathrm{d}\sigma}{\mathrm{d}t} = \mu_2\sigma - \alpha\rho^2 - a_2\sigma^3 - b_2\sigma\rho^2, \tag{6.72b}$$

$$\frac{\mathrm{d}\tilde{\chi}}{\mathrm{d}t} = \alpha\left(\frac{\rho^2}{\sigma} - 2\sigma\right)\tilde{\chi} - \frac{\hat{\beta}\sqrt{2}}{\rho}. \tag{6.72c}$$

As before, the ρ, σ-equations move from $\sigma \approx \sigma_0$, $\rho \approx 0$ to $\sigma \approx 0$, $\rho \approx \rho_0$, according to (6.72*a*) and (6.72*b*).

Solving for $\tilde{\chi}$ gives

$$\tilde{\chi} = \exp\left\{\int_t^T \left(2\alpha\sigma - \frac{\alpha\rho^2}{\sigma} + \frac{1}{T-t'}\right)\mathrm{d}t' - \ln(T-t)\right\}$$
$$\times\left(K + \int_t^T \frac{\hat{\beta}\sqrt{2}}{\rho}(T-t')\exp\left\{\int_{t'}^T \left(\frac{\alpha\rho^2}{\sigma} - 2\alpha\sigma - \frac{1}{T-t''}\right)\mathrm{d}t''\right\}\mathrm{d}t'\right), \tag{6.73}$$

where T is the semi-period, the time at which σ has its minimum value. T is determined by matching ρ. The constant K is determined by matching onto region (v). In both the H_+ and H_- cases, χ is negative as we enter region (v). Since we have a periodic orbit, the minimum value of σ is the same in region (v) as region (i), so the entry to region (v) is governed by

$$\chi \sim \frac{-\epsilon A_1}{\alpha\rho_0^2}\frac{1}{T-t}, \tag{6.74a}$$

$$\sigma \sim \alpha\rho_0^2|T-t|. \tag{6.74b}$$

Note that although on leaving region (iv) only half the orbit is complete, the other half is symmetric, so that σ has the same minimum value in regions (i) and (v). So considering (6.73) in the limit $t \to T^-$, we have

$$K = \frac{-A_1}{\alpha\rho_0^2} \tag{6.75}$$

since the second term tends to zero in this limit. Now we get a further matching condition by requiring that as $t \to -\infty$ in (6.73) we match on the asymptotic form of χ, (6.46*a*). From (6.73) and (6.75) we get

$$\chi \sim \exp\{2\alpha\sigma_0(T-t)\}\lim_{t_0\to-\infty}\exp\left\{\int_{t_0}^T \left(2\alpha(\sigma-\sigma_0) - \frac{\alpha\rho^2}{\sigma} + \frac{1}{T-t'}\right)\mathrm{d}t' - \ln(T-t_0)\right\}$$
$$\times\left(\frac{-\epsilon A_1}{\alpha\rho_0^2} + \lim_{t_0\to-\infty}\int_{t_0}^T \frac{\hat{\beta}\sqrt{2}}{\rho}(T-t')\exp\left\{\int_{t'}^T \left(\frac{\alpha\rho^2}{\sigma} - 2\alpha\sigma - \frac{1}{T-t''}\right)\mathrm{d}t''\right\}\mathrm{d}t'\right)$$
$$\sim \mp 2\exp -2\alpha\sigma_0(t-c_1). \tag{6.76}$$

From this we deduce that

$$\frac{-\epsilon A_1 I_4}{\alpha\rho_0^2}\exp 2\alpha\sigma_0 T + I_4 J_2 \exp 2\alpha\sigma_0 T = \mp 2 \exp 2\alpha\sigma_0 c_1,$$

where

$$J_2 = \int_{-\infty}^{T} \frac{(T-t')\sqrt{2}}{\rho} \exp\left[-2\alpha\sigma_0(T-t')\right] \times \lim_{t_0\to-\infty} \exp\left\{\int_{t_0}^{t'}\left(\frac{\alpha\rho^2}{\sigma} - 2\alpha(\sigma-\sigma_0) - \frac{1}{T-t''}\right)\mathrm{d}t''\right\}\mathrm{d}t'. \quad (6.77)$$

We now have all the matching results we need to determine ϵA_1 in terms of β.

Combining (6.70), (6.71) and (6.51) we get the semi-period

$$T = \frac{1}{(\mu_1 - b_1\sigma_0^2 + \alpha\sigma_0)} \log \frac{2}{I_1 I_2 I_3 \left|\frac{\epsilon A_1}{\alpha\rho_0^2} - \beta\right|}. \quad (6.78)$$

Inserting this in (6.77), and defining $\lambda = 2\alpha\sigma_0/(\mu_1 + \alpha\sigma_0 - b_1\sigma_0^2)$ as before, we get the equation

$$I_4 J_2 \beta - \frac{\epsilon A_1 I_4}{\alpha\rho_0^2} = \mp\frac{4}{I_1}\left(\frac{I_1 I_2 I_3}{2}\right)^{\lambda}\left|\frac{\epsilon A_1}{\alpha\rho_0^2} - \beta J_1\right|^{\lambda-1}, \quad (6.79)$$

which determines ϵA_1 in terms of β. It is clear from this that A_1 is an $O(1)$ quantity as required; putting it another way, the minimum value of σ, attained at $t = 0$, is $O(\beta)$. Note, however, from the above discussion that the minimum value of ρ near the singular point $\sigma = \sigma_0$, $\rho = 0$ is *not* $O(\beta)$ but is $O(\beta^{1/\lambda})$, somewhat larger. The period is $O(\ln 1/\beta)$.

In the H_+ case, we have the inequalities

$$\beta J_1 > \frac{\epsilon A_1}{\alpha\rho_0^2}, \quad \frac{\epsilon A_1}{\alpha\rho^2 0} > J_2\beta. \quad (6.80)$$

These clearly imply that

$$J_1 > J_2 \quad (6.81)$$

and it is also clear that since $\lambda - 1$ is positive there is a unique solution of (6.79) for A_1 with $\epsilon A_1/\alpha\rho_0^2$ lying between βJ_1 and βJ_2.

In the H_- case we have the inequalities

$$\frac{\epsilon A_1}{\alpha\rho_0^2} > \beta J_1, \quad J_2\beta > \frac{\epsilon A_1}{\alpha\rho_0^2}, \quad (6.82)$$

which imply that

$$J_1 < J_2. \quad (6.83)$$

Again in this case there is a unique solution for A_1.

The equations in region (vi) and (viii) are identical with those in regions (ii) and (iv) despite the change in sign in $\tilde{\chi}$ in these regions. This is because θ has changed by $\frac{1}{2}\pi$ in these regions also, so (6.66) holds in (vi) and (6.72*c*) holds in (viii). This symmetry requirement determines θ, since it is necessary for $\sin\theta$ to change sign when θ is reduced by $\frac{1}{2}\pi$. So

$$\sin\theta = -\sin(\theta - \tfrac{1}{2}\pi) \quad (6.84)$$

giving $\theta = \frac{1}{4}\pi$ and $\theta = \frac{5}{4}\pi$, which are the two cases H_+ and H_- respectively.

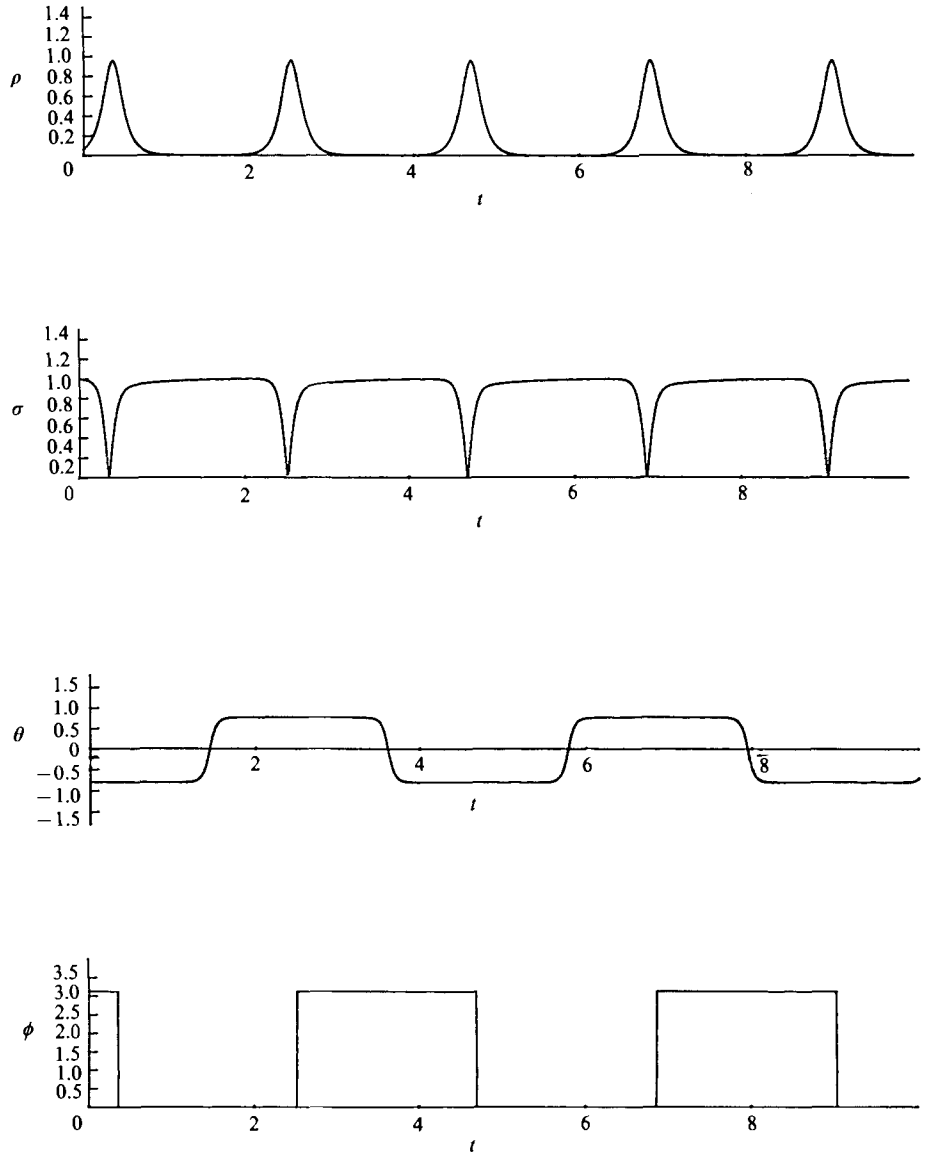

FIGURE 10. The homoclinic orbit rendered periodic by an imperfection. ρ, σ, θ and ϕ *vs.* time under system (6.63), (6.64) with $a_1 = a_2 = 1$, $b_1 = b_2 = 0$, $\mu_1 = 0.1$, $\mu_2 = 1.0$, $\alpha = 10$ and $\beta = 10^{-5}$.

The question of whether H_+ or H_- is the realized orbit depends on whether (6.81) or (6.83) holds. In the large-α limit (i.e. the scaling of §6.2 applies) the integrals I_1–I_4 and J_1 and J_2 can be evaluated explicitly. However, in this limit $J_1 = J_2$, and so the question of whether H_+ or H_- is realized depends on the higher-order terms. In numerical experiments, solutions of both types were found.

In summary, we have seen that the perturbation β has had the effect of resolving the degeneracy, giving a long (but finite) periodic orbit. The behaviour of ρ, σ, θ and ϕ as functions of time are shown in figure 10, in a case where the orbit is of the H_+ type.

7. Conclusion

We now consider the implications of the rich variety of behaviour at 2:1 resonance on our physical problem. Although the formal mathematical results apply strictly only to a small domain where the two modes come in at the same Rayleigh number, it is likely that the qualitative behaviour described here will have a reasonably large domain of relevance, as is often the case with weakly nonlinear theories. This certainly appears to be the case in cylindrical convection (Azouni & Normand 1983; Jones & Proctor 1987), where spatial resonance phenomena have been observed in the laboratory. However, in the cylindrical case the wavenumbers are quantized, so that the possibility of approximate, rather than exact, resonance does not occur. In this plane-layer problem, however, near resonance rather than exact resonance is a possibility if the apparatus is sufficiently long in the horizontal direction. Inclusion of this effect turns the amplitude equations into partial differential equations, with the possibility of soliton solutions (Coullet 1986). Analysis of near-resonance phenomena will be dealt with in a subsequent paper.

Perhaps the most remarkable feature to emerge from this study is the richness of the structure of the 2:1 resonance equations (5.1) compared to the non-resonant-interaction equations (1.2). We have concentrated in this paper on the case where the coefficients a_1 and a_2 are positive, as this condition obtains in the two-layer problem (see table 2): thermal convection is a supercritical phenomenon unless perturbing influences such as rotation or magnetic fields are present. There are, however, many problems where spatial resonance can occur that are subcritical, and for these a full analysis of (5.1) with a_1 or a_2 negative would be appropriate.

In all cases given in table 2, there are domains in the (μ_1, μ_2)-plane where we expect to see the pure mode (convection only in the thinner layer), the two mixed modes, M_+ and M_-, which represent steady convection in both layers, the travelling waves and the homoclinic orbit. The only qualitative difference in the two cases is in the stability of the modulated waves. In the cases where $G = 1$, so that simultaneous onset is achieved by having a more viscous liquid in the thicker layer, a_2 dominates a_1 and so $c = \frac{2}{9}(2a_1 - 2b_1 + b_2 - a_2)$ is negative (see (6.28) and below): in consequence, the modulated waves are unstable near the origin and may well be unstable everywhere. In the one-fluid case, however, a_1 dominates a_2, so that c is positive and modulated waves have a domain where they form a stable state. We note that in an experiment, it may not be easy to distinguish between a modulated wave an a homoclinic orbit rendered finite by imperfections (see §6.4).

The existence of the stable homoclinic orbit is itself slightly surprising, as it exists not just at a particular set of parameter values, like, for example, the homoclinic orbit in the Lorentz equations (Sparrow 1982), but over a whole region of the parameter space. One has to add additional terms, i.e. embed the system (5.1) in the system (6.62), in order to lift the degeneracy.

Although the two-layer model in Cartesian geometry is perhaps conceptually the simplest of problems involving spatial resonance, there are many other problems where the mathematics we have described is applicable. The step that involves most work is the calculation of the coefficients that appear in (5.1). For problems involving cylindrical or spherical geometry this is a larger undertaking than in the Cartesian case. However, the analysis probably has considerable application in these geometries, as there are problems where there is a parameter range where azimuthal wavenumbers $m = 1$ and $m = 2$ onset near each other, and system (5.1) is appropriate. The problem discussed in this paper achieves 2:1 resonance by having

instability due to the same mechanism in two distinct but coupled layers. But it is also possible to achieve resonance in one layer when two different instability mechanisms are present, such as shear instability and convection.

REFERENCES

AHLERS, G. & BEHRINGER, R. P. 1978 *Phys. Rev. Lett.* **40**, 772.

ARMBRUSTER, D., GUCKENHEIMER, J. & HOLMES, P. 1987 *Physica D* (in press).

AZOUNI, M. A. & NORMAND, C. 1983 *Geophys. Astrophys. Fluid Dyn.* **23**, 223–245.

BUSSE, F. H. & OR, A. C. 1986 *Z. Angew. Math. Phys.* **37**, 608–623.

BUSSE, F. H. & WHITEHEAD, J. A. 1971 *J. Fluid Mech.* **47**, 305–320.

CHANDRASEKHAR, S. 1961 *Hydrodynamic and Hydromagnetic Stability.* Oxford University Press.

CHATÉ, H. & MANNEVILLE, P. 1987 *Phys. Rev. Lett.* **58**, 112–115.

COULLET, P. 1986 *Cont. Math.* **56**, 724.

CROSS, M. C. & NEWELL, A. C. 1984 *Physica D*, **10**, 299–328.

DANGELMAYR, G. 1986 *Dyn. Stab. Systems* 1, 159–185.

DANGELMAYR, G. & ARMBRUSTER, D. 1986 *Cont. Math.* **56**, 53–68.

FAUVE, S. 1985 *Woods Hole Oceanographic Institution Technical Rep.* WHOI-85-36, pp. 55–70.

JONES, C. A. & PROCTOR, M. R. E. 1987 *Phys. Lett. A* **121**, 224–228.

KNOBLOCH, E. & GUCKENHEIMER, J. 1982 *Phys. Rev. A.* **27**, 408–417.

KNOBLOCH, E. & PROCTOR, M. R. E. 1981 *J. Fluid Mech.* **108**, 291–316.

KNOBLOCH, E. & PROCTOR, M. R. E. 1988 *Proc. R. Soc. Lond.* A **415**, 61–90.

KOLODNER, P., PASSNER, A., SURKO, C. M. & WALDEN, R. W. 1986 *Phys. Rev. Lett.* **56**, 2621.

MALKUS, W. V. R. & VERONIS, G. R. 1958 *J. Fluid Mech.* **4**, 225–260.

NEWELL, A. C. & WHITEHEAD, J. A. 1968 *J. Fluid Mech.* **38**, 279–303.

POMEAU, Y. 1984 *Cellular Structures in Instabilities* (ed. J. E. Wesfreid & S. Zaleski). Lecture Notes in Physics, vol. 210, pp. 207–214. Springer.

RAYLEIGH, LORD 1916 *Phil. Mag.* (6) **32**, 529.

ROSENBLAT, S., DAVIS, S. H. & HOMSY, G. M. 1982 *J. Fluid Mech.* **120**, 91–138.

SEGEL, L. A. 1962 *J. Fluid Mech.* **14**, 97–114.

SEGEL, L. A. 1965 *J. Fluid Mech.* **21**, 359–384.

SPARROW, C. 1982 *The Lorenz Equations: Bifurcations, Chaos and Strange Attractors.* Springer.